NEOPLASIA
www.neoplasia.com

Volume 15 Number 8 August 2013 pp. 875–887 875

Host Matrix Modulation by Tumor Exosomes Promotes Motility and Invasiveness[1,2]

Wei Mu*, Sanyukta Rana* and Margot Zöller*,†

*Department of Tumor Cell Biology, University Hospital of Surgery, Heidelberg, Germany; †German Cancer Research Center, Heidelberg, Germany

Abstract

Exosomes are important intercellular communicators, where tumor exosomes (TEX) severely influence hematopoiesis and premetastatic organ cells. With the extracellular matrix (ECM) being an essential constituent of non-transformed tissues and tumors, we asked whether exosomes from a metastatic rat tumor also affect the organization of the ECM and whether this has consequences on host and tumor cell motility. TEX bind to individual components of the ECM, the preferential partner depending on the exosomes' adhesion molecule profile such that high CD44 expression is accompanied by hyaluronic acid binding and high $\alpha_6\beta_4$ expression by laminin (LN) 332 binding, which findings were confirmed by antibody blocking. TEX can bind to the tumor matrix already during exosome delivery but also come in contact with distinct organ matrices. Being rich in proteases, TEX modulate the ECM as demonstrated for degradation of collagens, LNs, and fibronectin. Matrix degradation by TEX has severe consequences on tumor and host cell adhesion, motility, and invasiveness. By ECM degradation, TEX also promote host cell proliferation and apoptosis resistance. Taken together, the host tissue ECM modulation by TEX is an important factor in the cross talk between a tumor and the host including premetastatic niche preparation and the recruitment of hematopoietic cells. Reorganization of the ECM by exosomes likely also contributes to organogenesis, physiological and pathologic angiogenesis, wound healing, and clotting after vessel disruption.

Neoplasia (2013) 15, 875–887

Introduction

Tumors depend on a cross talk with the surrounding [1] to guarantee survival (angiogenesis, immune escape) [2,3], for phenotypic changes (epithelial-to-mesenchymal transition) required to leave the primary tumor mass [4], and for preparing the bone marrow and premetastatic organs allowing migrating tumor cells to settle and grow [5]. Recently, evidence is accumulating that this tumor cell–host cross talk, which includes long distance communication, mostly relies on tumor exosomes (TEX) [6–9].

Exosomes are small vesicles delivered by many cells in the organism and abundantly by thrombocytes and tumor cells [10]. Exosomes derive from early endosomes, which fuse to multivesicular bodies, from where the individual vesicles are released as exosomes in the extracellular space [11–14]. Accordingly, the exosomal protein profile is rich in molecules located in membrane domains prone for internalization such as rafts and tetraspanin-enriched microdomains as well as molecules engaged in fission, scission, and vesicular transport, adhesion molecules, and proteases [14–17]. Exosomes also harbor mRNA and miRNA [18], where the delivery of miRNA may be the most important factor in target cell modulation [18–21]. Nonetheless, the exosomal membrane takes over an important function in binding and uptake by selected target cells, where exosomal annexins, adhesion molecules, and tetraspanins are involved [13,22,23]. For dendritic cells, it is known that they can be replaced by exosomes, which provide peptide-loaded major histocompatibility complex (MHC) and co-stimulatory molecules

Abbreviations: ASML, BSp73ASML; ASML-CD44v^{kd}, ASML cells with a stable knockdown of CD44v4-v7; CM, conditioned medium; CM^{-exo}, exosome-depleted CM; coll, collagen; ECM, extracellular matrix; EGF, epidermal growth factor; FGF, fibroblast growth factor; FN, fibronectin; HA, hyaluronic acid; LN, laminin; LnStr, lymph node stroma cells; LuFb, lung fibroblasts; R, receptor; RAEC, rat aortic endothelial cells; TEX, tumor exosomes

Address all correspondence to: Prof Margot Zöller, MD, Department of Tumor Cell Biology, University Hospital of Surgery, Im Neuenheimer Feld 365, D 69120 Heidelberg, Germany. E-mail: margot.zoeller@uni-heidelberg.de

[1]This work was supported by the NCT Interdisciplinary Research Program (M.Z.) and the NES Program of the University of Karlsruhe (M.Z.). All authors declare no conflict of interest.

[2]This article refers to supplementary materials, which are designated by Tables W1 and W2 and Figures W1 to W4 and are available online at www.neoplasia.com.

Received 6 April 2013; Revised 1 May 2013; Accepted 13 May 2013

DOI 10.1593/neo.13786

[24,25] and exosomal heat shock proteins that support non-adaptive immune responses [26,27]. Finally, exosomes are rich in proteases that are functionally active [28–31]. This has been explored for the impact of exosomal proteases on the protein profile of exosomes, the release of cytokines and soluble receptors [31–34], though to our knowledge the impact of exosomal proteases on the extracellular matrix (ECM) has not yet been explored.

We showed in a rat pancreatic adenocarcinoma model [35,36] that exosomes are an important factor in premetastatic niche preparation [37]. A CD44v4-v7^{kd} of the highly metastatic BSp73ASML tumor line (ASML^{wt}, ASML-CD44v^{kd}) poorly metastasizes but gains in metastatic capacity, when rats are pretreated with conditioned medium (CM) of the ASML^{wt} line. While exosome-depleted CM (CM^{-exo}) does not promote metastasis and exosomes by themselves exert a weak effect, a mixture of ASML^{wt} CM^{-exo} with exosomes accelerates metastasis formation [37]. This finding pointed toward a possible cross talk of exosomes not only with stroma cells but also with the tumor and/or host matrix. We here explored this question for the matrix of non-transformed lymph node stroma (LnStr) and lung fibroblasts (LuFb) as lymph nodes and lungs are the metastatic organs of ASML cells [35]. TEX have a strong impact on the stroma cell matrix, which supports stroma cell motility and invasiveness.

Materials and Methods

Cell Lines

The rat pancreatic adenocarcinoma lines BSp73ASML (ASML^{wt}) [35] and BSp73ASML-CD44v4-v7^{kd} (ASML-CD44v^{kd}) [36], a rat aortic endothelial cell line (RAEC), a rat lung fibroblast line (LuFb), and a rat lymph node stroma line (LnStr) [38] are maintained in RPMI 1640/10% fetal calf serum (FCS). Culture medium of ASML-CD44v^{kd} contains, in addition, 750 μg/ml G418. Confluent cultures are detached with trypsin or EDTA and split.

Antibodies

Antibodies are listed in Table W1.

Exosome Preparation

Cells were cultured (48 hours) in serum-free medium. Cleared supernatants (2 × 10 minutes, 500*g*; 1 × 20 minutes, 2000*g*; 1 × 30 minutes, 10,000*g*) were ultracentrifuged (90 minutes, 100,000*g*) and washed [phosphate-buffered saline (PBS), 90 minutes, 100,000*g*]. The supernatant was collected as CM^{-exo}. The pellet was resuspended (10 ml of PBS), layered on 10 ml of 40% sucrose, and centrifuged (90 minutes, 100,000*g*). The top layer was removed, and the sucrose layer was diluted with PBS and centrifuged (90 minutes, 100,000*g*). Where indicated, exosomes were rhodamine-DHPE– or SP-Dio$_{18}$ (3)–labeled (1:10,000 dilution; Invitrogen, Karlsruhe, Germany; 30 minutes, 4°C) before sucrose gradient centrifugation and two washings (90 minutes, 100,000*g*). Relative fluorescence intensity was evaluated at 540-nm excitation, 590-nm emission or 497-nm excitation, 513-nm emission (Fluoroskan Ascent; Thermo Scientific, Karlsruhe, Germany) and adjusted to rhodamine-DHPE or SP-Dio$_{18}$(3) standards.

Western Blot

CM (200 μg) or exosomes (100 μg) were lysed (Hepes buffer, 1% Lubrol or 1% Brij96, 1 mM PMSF, protease inhibitor mix, 30 minutes, 4°C). Lysates were resolved on 7% to 12% sodium dodecyl sulfate–polyacrylamide gel electrophoresis (non-reducing). After transfer, blocking, and immunoblot analysis with primary and HRP-labeled streptavidin or secondary antibodies, blots were developed with the enhanced chemiluminescence (ECL) detection system.

Flow Cytometry

Flow cytometry followed routine procedures; for intracellular staining, cells were fixed and permeabilized in advance. Dye-labeled exosomes were incubated with 4-μm aldehyde-sulfate latex beads (Invitrogen). Where indicated, latex beads (1 μl) were coated with antibody or matrix proteins (10 μg/ml) blocking free aldehyde groups [PBS/100 mM glycine, 20 minutes, room temperature (RT)] before incubation with exosomes. In blocking studies, exosomes were preincubated with antibody and non-bound antibody was removed by washing and ultracentrifugation. Samples were analyzed in a FACSCalibur using the CellQuest program.

Immunofluorescence

Cells were seeded on glass cover slides and stained with the indicated antibody. Alternatively, dye-labeled exosomes (15 μl, 40 μg/ml) were seeded on matrix protein–coated slides (Table W2) or exosomes (10 μg) were incubated with CM^{-exo} (100 μg) for 24 hours at 37°C. Free exosomes were removed by ultracentrifugation. CM with bound exosomes was seeded on glass cover slides. Coated cover slides were counterstained with matrix protein–specific antibodies. Digitized images were generated using a Carl Zeiss LSM710 confocal microscope and Carl Zeiss Axioview Rel. 4.6 software. Quantification of fluorescence intensity was performed with the ImageJ program.

Enzyme-linked Immunosorbent Assay

Dye-labeled exosomes were incubated for 24 hours in F-bottom 96-well plates that had been coated with CM or matrix proteins. Free exosomes were removed by washing. The content of matrix-bound exosomes was evaluated in a fluorescence ELISA reader (Fluoroskan Ascent; Thermo Scientific).

Protease Activity

Exosomes (20 μg) were incubated with matrix proteins (1 μg) or CM^{-exo} (50 μg) for 24 hours. After dissolving in Laemmli buffer and sodium dodecyl sulfate–polyacrylamide gel electrophoresis separation, matrix protein degradation was evaluated by Western blot (WB) or zymography (separation in a 10% acrylamide/1 mg/ml gelatin gel, washing, and Coomassie Blue staining).

Adhesion Assay

Cells (2×10^4/100 μl) were seeded on matrix protein–coated F-bottom 96-well plates for 2 hours at 37°C. After washing, adherent cells were stained with crystal violet and dissolved in 10% acetic acid, evaluating staining intensity photometrically. Adhesion is presented as percentage of seeded cells.

Cell Migration and Invasion

Cells (5×10^3 in 40 μl) were seeded in the upper part of a Boyden chamber in 30 μl of RPMI/0.1% BSA. The lower part, separated by an 8-μm pore size polycarbonate membrane (Neuroprobe, Gaithersburg, MD), contained 30 μl of RPMI/20% FCS or CM^{-exo} with/without exosomes (10 μg/ml). Migration was evaluated after 16 hours by staining the lower membrane side with crystal violet, measuring $OD_{595\ nm}$ after lysis. Migration is presented as percentage of input cells. For invasion, matrigel was mixed (1:1) with RPMI 1640 or TEX and

incubated for 24 hours at 37°C. Thereafter, matrigel was seeded on the lower membrane site of a transwell insert. LuFb, LnStr, and RAEC (5×10^4) were layered on the upper site of the insert. After 24 hours, cells at the upper site of the membrane were removed. Cells within the matrigel were documented by light microscopy and were counted.

For video microscopy, Hoechst 33342–stained tumor cells (5×10^4) were mixed with CM^{-exo} pretreated for 24 hours with exosomes. Cell migration in untreated or exosome-pretreated CM^{-exo} was evaluated for 24 hours using an Olympus IX81 inverse microscope with an Hg/Xe lamp, an incubation chamber (37°C, 5% CO_2), a charge-coupled device (CCD) camera (Hamamatsu, Herrsching, Germany), and a ScanR acquisition software (Olympus, Hamburg, Germany). Two pictures (20-fold magnification) per chamber (2-millisecond exposure) were taken every 20 minutes for 12 hours. Migration was quantified according to Manual_tracking plugin (F.P. Cordeliére, Centre de Recherche de l'Institute Curie) running in the open-source software ImageJ. Path length of 20 individual cells in each setting was calculated for every 15 minutes by customized programs. The mean pathway length per 1 hour is presented.

Animal Experiments

BDX rats (five per group) received 400 µl of matrigel subcutaneously (s.c.). Where indicated, matrigel was pretreated at 37°C for 24 hours with 100 µg of $ASML^{wt}$ or ASML-$CD44v^{kd}$ exosomes. Rats were sacrificed after 5 days to excise the matrigel pellet, which was shock frozen for immunohistochemistry. To control for TEX binding to the ECM, rats (three per group) received an intravenous (i.v.) injection of 400 µg of SP-Dio_{18}(3)–labeled $ASML^{wt}$ or ASML-$CD44v^{kd}$ exosomes. Rats were sacrificed after 48 hours. Organs were excised, shock frozen, and analyzed using a confocal microscope for the recovery of exosomes, particularly those attached to the ECM. Metastatic ASML growth after intrafootpad injection was evaluated in shock-frozen tissue sections after autopsy.

Statistical Analysis

P values < .05 (two-tailed Student *t* test, analysis of variance) were considered significant.

Results

Exosomes are appreciated as important intercellular communicators [14]. We here explored whether exosomes also communicate with the ECM. Using TEX as a model, we evaluated whether exosomes modulate the host matrix to favor cell motility, activation, and survival.

TEX Bind to the Host Matrix

Exosomes were derived from the metastatic rat pancreatic adenocarcinoma ASML [35] or the poorly metastatic ASML-$CD44v^{kd}$ line [36]. Tumor cells, LnStr, and LuFb as well as CM^{-exo} derived thereof contain matrix proteins, with tenascin, vitronectin (VN), and fibronectin (FN) being abundant in LnStr and LuFb CM^{-exo}, coll II in LnStr, and coll IV in LuFb CM^{-exo} (Figure W1). Using dye-labeled exosomes revealed binding to matrix protein–coated latex beads. Major differences in binding to individual matrix proteins was not observed. However, binding of ASML-$CD44v^{kd}$ exosomes was weaker, particularly binding to hyaluronic acid (HA; Figure 1*A*). TEX also bind to their own as well as to stroma cell CM^{-exo}, the ASML-$CD44v^{kd}$ CM^{-exo} exerting strongly reduced binding capacity (Figure 1, *B–D*), supporting a non-random process. Importantly, demonstrated for i.v. injected dye-labeled TEX, exosomes also bind *in vivo* to selected matrices, particularly of skeletal muscles, heart, lung, and vessels. Though, due to the ECM being composed of mixtures of matrix proteins, counterstaining of matrix proteins did not allow for a clear coordination of TEX to individual matrix proteins, there is strong evidence for collagen (coll) and laminin (LN) binding (Figures 1*E* and W2).

Being concerned about the potential functional relevance of TEX binding to selected matrices, we noted that ASML cells, though preferentially metastasizing through the lymphatic system to the lung, may settle and grow along the basal lamina of the skin without invading the epidermis or forming solid tumor nodules (data not shown). Similarly, without destroying the muscle, ASML cells invade and grow along the basement membrane of muscles (Figure 1*F*), both the lamina basalis of the skin and the basement membrane surrounding skeletal myofibers being strong attractants for ASML-TEX.

Exosomes bind to matrix proteins through adhesion molecule receptors. ASML exosomes express CD49c and CD44 at a high level and $\alpha_6\beta_4$ at a medium high level (Figure 1*G*). Exosomes were preincubated with antibody against these highly expressed adhesion molecules and non-bound antibodies were removed by ultracentrifugation before evaluating exosome binding to matrix protein–coated latex beads. As demonstrated for coll IV, FN, LN111, and HA binding, antibody preincubation of exosomes significantly affected binding, the strongest reduction being provoked by anti-CD49c toward LN111 and by anti-CD44 toward HA (Figure 1*H*).

Taken together, exosome binding to the ECM is a non-random process that varies depending on the composition of the host/tumor cell matrix and the adhesion molecule profile of the exosomes. Importantly, TEX binding to selected matrices appears to attract tumor cells and/or to facilitate tumor cell migration along TEX-decorated matrices. Thus, the question arose on the impact of bound TEX on the host matrix.

Host Matrix Modulation by TEX

Exosomes are rich in proteases, and exosomal proteases are functionally active [28–31]. $ASML^{wt}$ exosomes are rich in uPAR, MMP3, ADAM17 (TACE), ADAMTS1, ADAMTS8, and CD13. The protease profile of ASML-$CD44v^{kd}$ exosomes differs for uPAR, MMP9, MMP13, and ADAM17, which are less abundant, whereas HAdase is enriched [37,39] (Figure 2, *A–C*). Having demonstrated functional activity of exosomal MMP2 and MMP9 by zymography (Figure 2*D*), we evaluated matrix protein degradation by $ASML^{wt}$ and ASML-$CD44v^{kd}$ exosomes. Coll II is degraded by $ASML^{wt}$ and ASML-$CD44v^{kd}$ exosomes. Coll I, coll IV, LN111, LN332, and FN were more efficiently degraded by $ASML^{wt}$ exosomes. VN was hardly degraded (Figure 2*E*). As demonstrated for FN, tenascin, VN, LN111, LN332, and coll I, upon co-incubation of LnStr-, LuFb-, and RAEC-CM^{-exo}, TEX efficiently degrade naturally organized matrix proteins, where $ASML^{wt}$ exosomes display higher efficacy particularly in LN and coll I degradation (Figure 2*F*).

Thus, TEX modulate the stroma matrix by matrix protein degradation.

The Exosome-Modulated ECM Promotes Stroma Cell Migration and Invasiveness

The ECM is not only a static scaffold that keeps cells in their organ context but also plays an important role in tissue remodeling. This poses the question of whether the TEX-modulated stroma matrix better serves the demands of metastasizing tumor cells.

When controlling for cell shape on the stroma matrix depending on TEX modulation, cell shape was not strikingly altered, but focal adhesion points were more pronounced, when cells were incubated

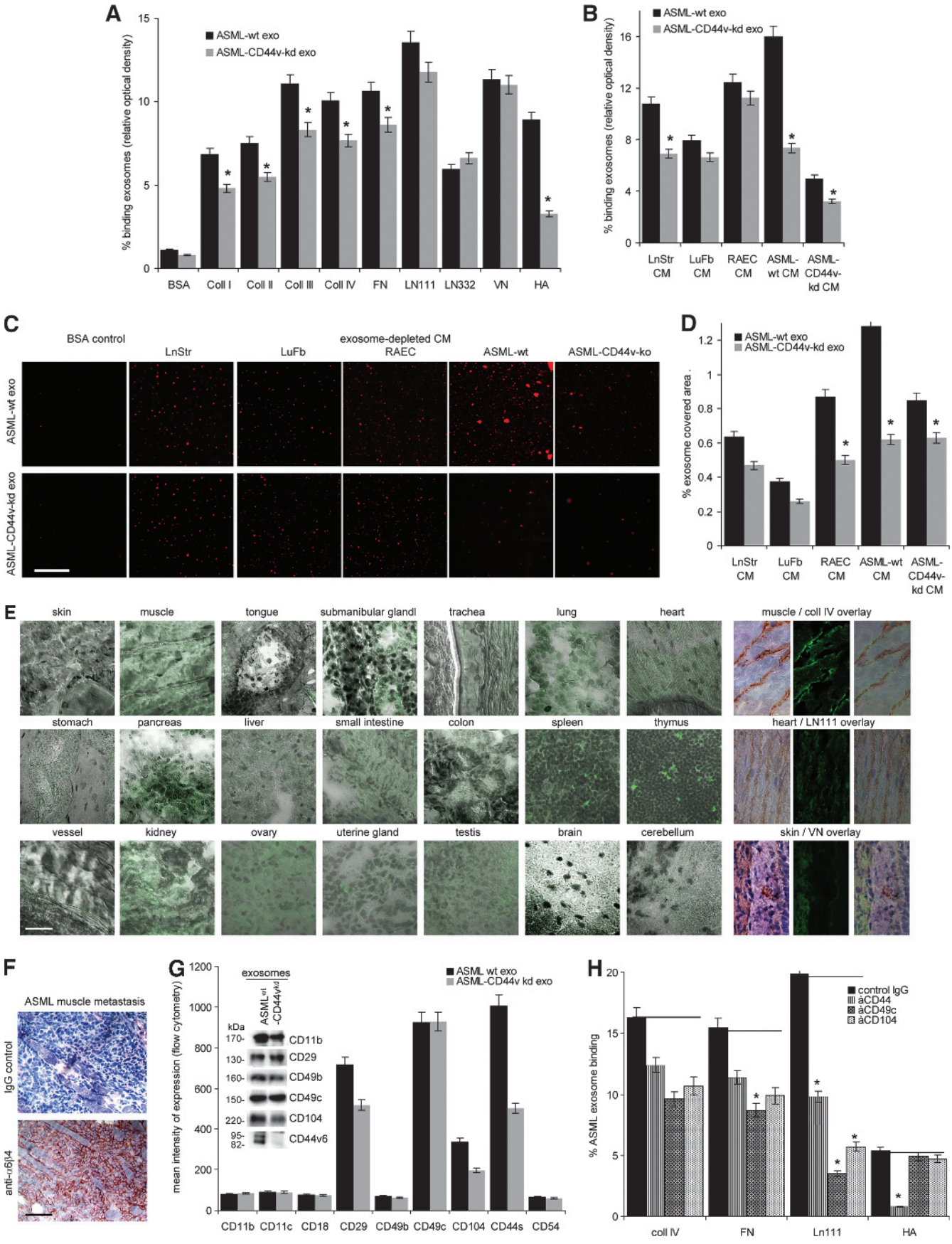
A
% binding exosomes (relative optical density)
ASML-wt exo
ASML-CD44v-kd exo
BSA
Coll I
Coll II
Coll III
Coll IV
FN
LN111
LN332
VN
HA
B
% binding exosomes (relative optical density)
ASML-wt exo
ASML-CD44v-kd exo
LnStr CM
LuFb CM
RAEC CM
ASML-wt CM
ASML-CD44v-kd CM
C
BSA control
exosome-depleted CM
LnStr
LuFb
RAEC
ASML-wt
ASML-CD44v-ko
ASML-wt exo
ASML-CD44v-kd exo
D
% exosome covered area
ASML-wt exo
ASML-CD44v-kd exo
LnStr CM
LuFb CM
RAEC CM
ASML-wt CM
ASML-CD44v-kd CM
E
skin
muscle
tongue
submanibular glandl
trachea
lung
heart
muscle / coll IV overlay
stomach
pancreas
liver
small intestine
colon
spleen
thymus
heart / LN111 overlay
vessel
kidney
ovary
uterine gland
testis
brain
cerebellum
skin / VN overlay
F
ASML muscle metastasis
IgG control
anti-α6β4
G
mean intensity of expression (flow cytometry)
exosomes
ASML wt exo
ASML-CD44v kd exo
kDa
CD11b
CD29
CD49b
CD49c
CD104
CD44v6
CD11b CD11c CD18 CD29 CD49b CD49c CD104 CD44s CD54
H
% ASML exosome binding
control IgG
áCD44
áCD49c
áCD104
coll IV
FN
Ln111
HA

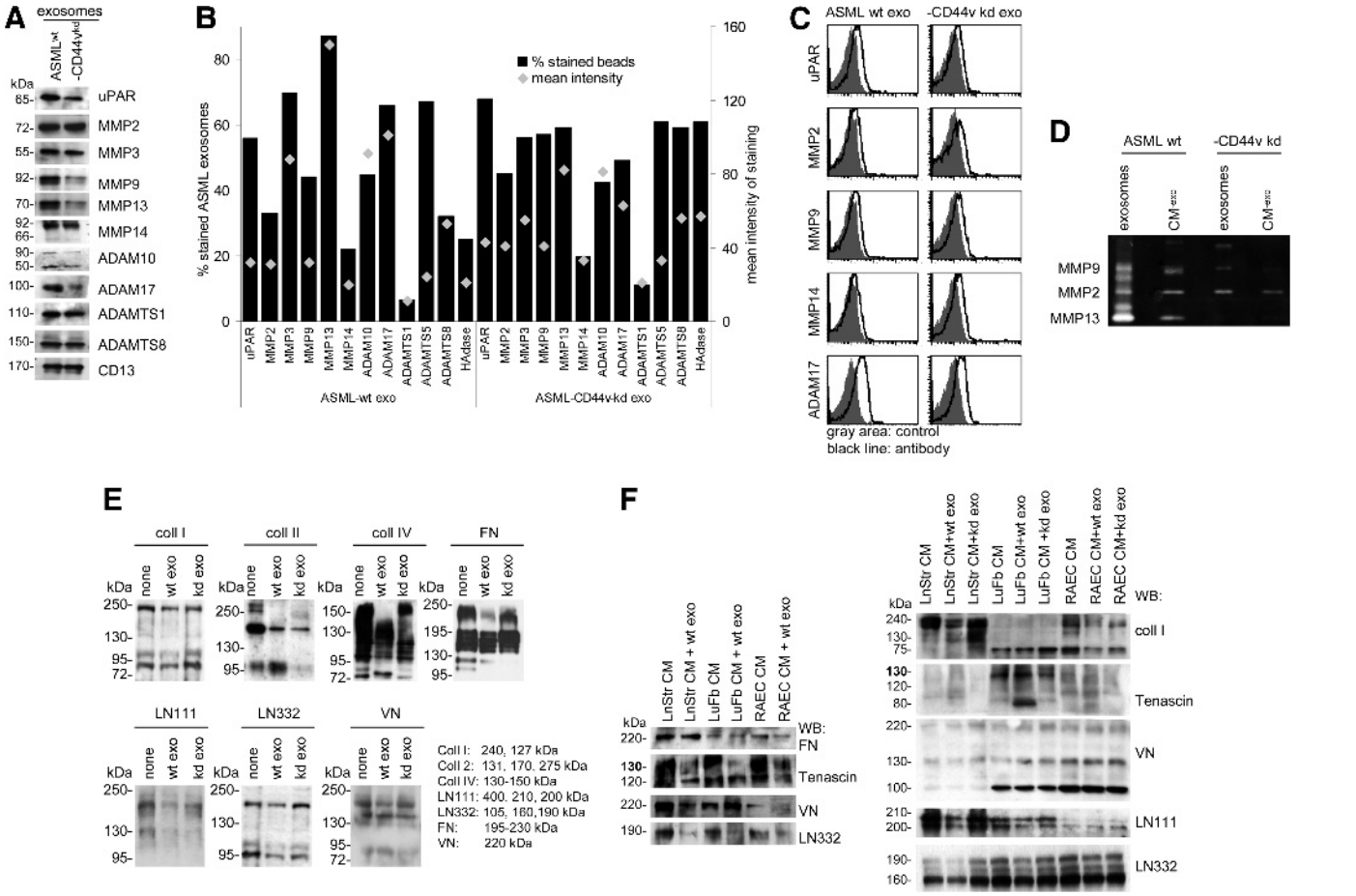

Figure 2. Exosomes and matrix degradation. (A) Matrix-degrading enzymes in ASML^{wt} and ASML-CD44v^{kd} exosomes were evaluated by WB and flow cytometry, (B) mean values of triplicates (percentage of stained beads and mean intensity of staining), and (C) representative examples. (D) Zymography of ASML^{wt} and ASML-CD44v^{kd} CM^{-exo} and exosomes. (E and F) WB of matrix proteins, LnStr-CM^{-exo}, LuFb-CM^{-exo}, and RAEC CM^{-exo} after co-culture with ASML^{wt} and ASML-CD44v^{kd} exosomes. Blots were incubated with the indicated antibodies. The expected size of matrix proteins and breakdown products is indicated. Coll II is degraded by ASML^{wt} and ASML-CD44v^{kd} exosomes. Coll I, coll IV, FN, LN111, and LN332 are more efficiently degraded by ASML^{wt} than ASML-CD44v^{kd} exosomes. This accounts for purified matrix proteins and the stroma cell matrix.

on TEX-modulated matrices, independent on whether the matrix derived from the tumor or the host cell (Figures W3 and 3*A*). In line with this finding, there has been a slight increase in adhesion to the donor matrix when modulated by ASML exosomes. This accounted particularly for LuFb and RAEC, ASML^{wt} exosomes exerting a stronger effect than ASML-CD44v^{kd} exosomes (Figure 3*B*). More striking has been the impact on migration. Transwell migration of LnStr, LuFb, and RAEC was significantly strengthened when the autologous CM was preincubated with ASML^{wt} exosomes, whereas ASML^{kd} exosomes did not exert a considerable effect (Figure 3*C*). Increased migration

Figure 1. Exosome binding to matrix proteins. (A–D) Dye-labeled ASML^{wt} and ASML-CD44v^{kd} exosomes were incubated with (A) matrix protein–coated latex beads or (B) matrix protein– or (C and D) CM^{-exo}-coated ELISA plates or glass slides. Exosome binding was evaluated by (A) flow cytometry, (B) OD, and (C and D) confocal microscopy. (A, B, and D) Mean values ± SD of triplicates and (C) representative examples are shown (scale bar, 10 μm). (E) Dye-labeled ASML^{wt} and ASML-CD44v^{kd} exosomes (200 μg) were i.v. injected. Rats were sacrificed after 48 hours, and organs were excised and shock frozen. Tissue sections were counterstained with hematoxylin and eosin (H&E), evaluating recovery of exosomes by confocal microscopy. For selected samples, overlays with immunohistochemistry staining for matrix proteins are shown (scale bar, 10 μm). (F) BDX rats received ASML cells intrafootpad. Abdominal wall muscle was excised at autopsy and shock frozen. Tissue sections were stained with control IgG or B5.5 (anti-$\alpha_6\beta_4$; scale bar, 20 μm). (G) Flow cytometry and WB analysis of adhesion molecule expression on ASML^{wt} and ASML-CD44v^{kd} exosomes. (H) Dye-labeled exosomes were incubated with the indicated antibodies. Non-bound antibodies were removed by centrifugation (90 minutes, 100,000*g*). Exosomes (pellet) were collected and incubated with the indicated matrix proteins coated on ELISA plates. After 2 hours at 4°C, non-bound exosomes were removed by washing and fluorescence intensity (% of total exosomes) was evaluated. Means ± SD of triplicates are shown. Significant inhibition of exosome binding is indicated by an asterisk. Exosomes selectively bind matrix proteins and tissue matrices through adhesion receptors *in vitro* and *in vivo*, where TEX-decorated matrices appear to attract tumor cells.

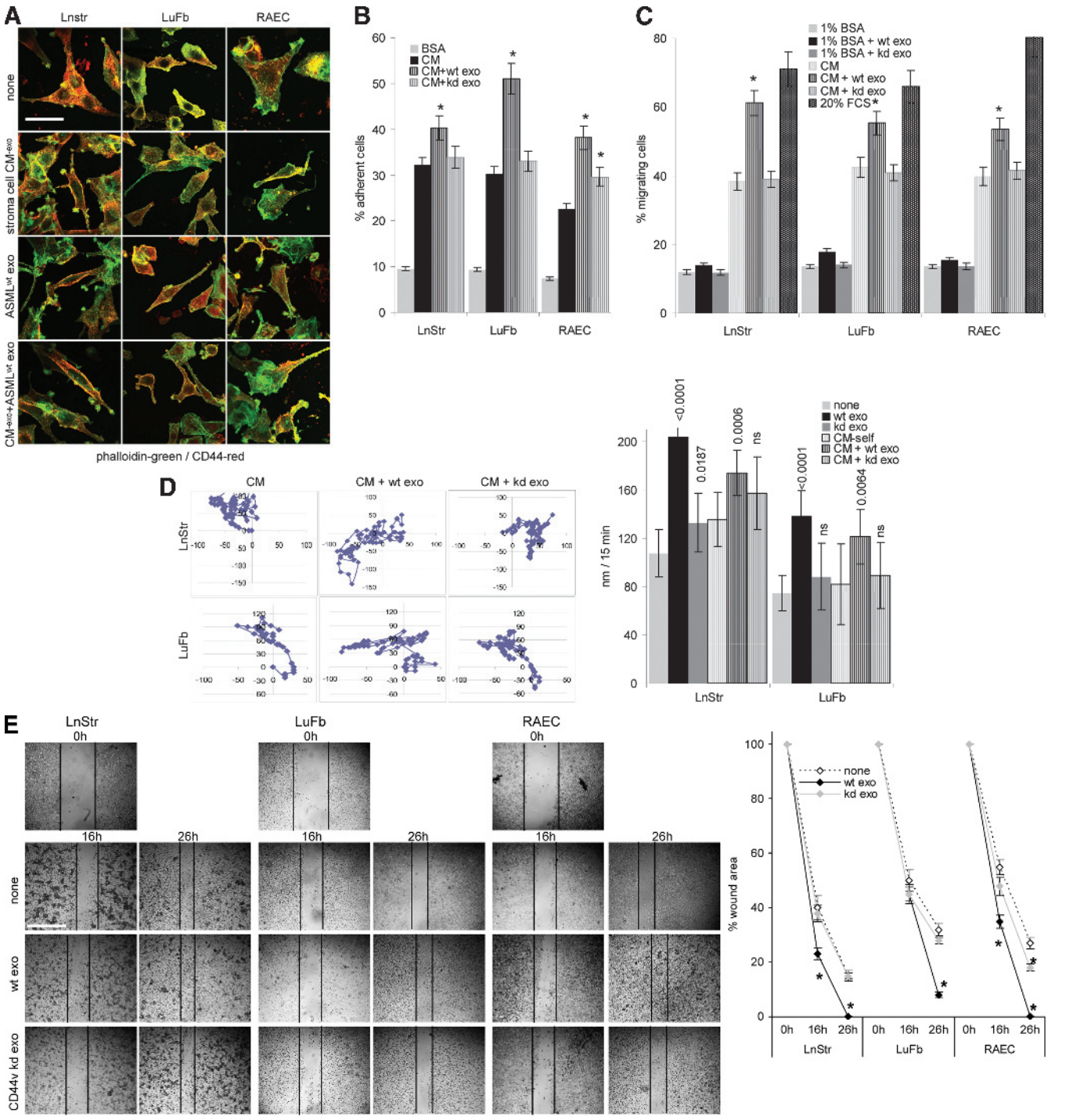

Figure 3. TEX-modulated CM and cell adhesion/motility. (A) Cells were seeded on cover slides coated with BSA, CM^{-exo}, or $ASML^{wt}$ exosome–treated CM^{-exo} and were stained with phalloidin–fluorescein isothiocyanate (FITC) and anti–CD44-Cy3, where indicated cultures contained $ASML^{wt}$ exosomes. Representative examples (confocal microscopy; scale bar, 100 μm) are shown. (B) LnStr, LuFb, and RAEC were seeded on BSA, CM^{-exo}, or CM^{-exo} plus $ASML^{wt}$ or ASML-$CD44v^{kd}$ exosome–coated 96-well plates. Adhesion was evaluated after 2 hours (crystal violet staining of adherent cells). The mean ± SD of the percent adherent cells is shown. (C) Cells were seeded in the upper part of a Boyden chamber, and the lower part contained BSA, 20% FCS, or CM^{-exo} pretreated with $ASML^{wt}$ or ASML-$CD44v^{kd}$ exosomes as indicated. Migration was evaluated after 16 hours by crystal violet staining of the lower membrane site. Mean values (triplicates) ± SD of the percentage of migrating cells are shown. (D) Cells were seeded on CM^{-exo} or TEX-pretreated CM^{-exo}. Cell migration was observed for 24 hours. Representative examples and the mean ± SD track of 10 cells per 15 minutes are shown. (E) Cells were seeded on plates coated with CM^{-exo} or TEX-pretreated CM^{-exo}. Subconfluent monolayers were scratched with a pipette tip and wound closure was followed for 26 hours. Representative examples (scale bar, 250 μm) and mean ± SD (three wells) of wound closure are shown. (B–E) Significant differences between CM^{-exo} and TEX-pretreated CM^{-exo} are shown or indicated by asterisk. The TEX-modulated stroma matrix promotes stroma cell motility.

was confirmed by video microscopy, where migration of LuFb and LnStr on their own matrix was nearly doubled in the presence of ASML^{wt} exosomes but increased only about 1.2-fold in the presence of ASML-CD44v^{kd} exosomes (Figure 3*D*). *In vitro* wound healing of LnStr, LuFb, and RAEC was also significantly accelerated in the presence of ASML^{wt} exosomes (Figure 3*E*).

Finally, we asked whether TEX would also modulate the matrix to support invasiveness. Matrigel was co-cultured with ASML^{wt} and ASML-CD44v^{kd} exosomes for 16 hours. Thereafter, LuFb, LnStr, or RAEC were added and matrigel invasion was evaluated after 24 hours. Matrigel invasion by LuFb and RAEC was strikingly increased in ASML^{wt} exosome–modulated matrigel. LnStr, spontaneously not invading the matrigel, did so after matrigel modulation by ASML^{wt} exosomes. ASML-CD44v^{kd} exosomes exerted no or a much weaker effect (Figure 4*A*). Fittingly, 7 days after s.c. injection of a matrigel plug, fibroblasts (vimentin^{+}) and endothelial cells (CD31^{+}) were recovered in the plug only when pretreated with exosomes, ASML^{wt} exosomes exerting a more pronounced effect than ASML-CD44v^{kd} exosomes (Figure 4*B*).

Taken together, the TEX-modulated host matrix supports host cell migration and strongly facilitates invasiveness.

The Exosome-Modulated ECM Supports Stroma Cell Proliferation and Apoptosis Resistance

We and others demonstrated before the feedback of the tumor matrix, inherently modulated by TEX, on the tumor cell [39–42]. Thus, it became likely that the TEX-modulated host matrix may also affect host cells. The inherently exosome-modulated ASML^{wt} matrix supports LuFb and LnStr, weakly LNC and BMC, but not RAEC proliferation. The ASML^{kd} matrix also exerted a weak effect on LnStr, LuFb, and LNC cells (Figure 5*A*). An even stronger growth-promoting stimulus was exerted on LnStr, LuFb, and RAEC upon modulation of their own matrix by TEX (Figure 5*B*). Accelerated growth of LnStr, LuFb, and RAEC is accompanied by up-regulation of CXCR4, epidermal growth factor receptor (EGFR), fibroblast growth factor receptor (FGFR; only LnStr), PDGFR (only LuFb), and vascular endothelial growth factor receptor 1 (VEGFR1), where in most instances the effect

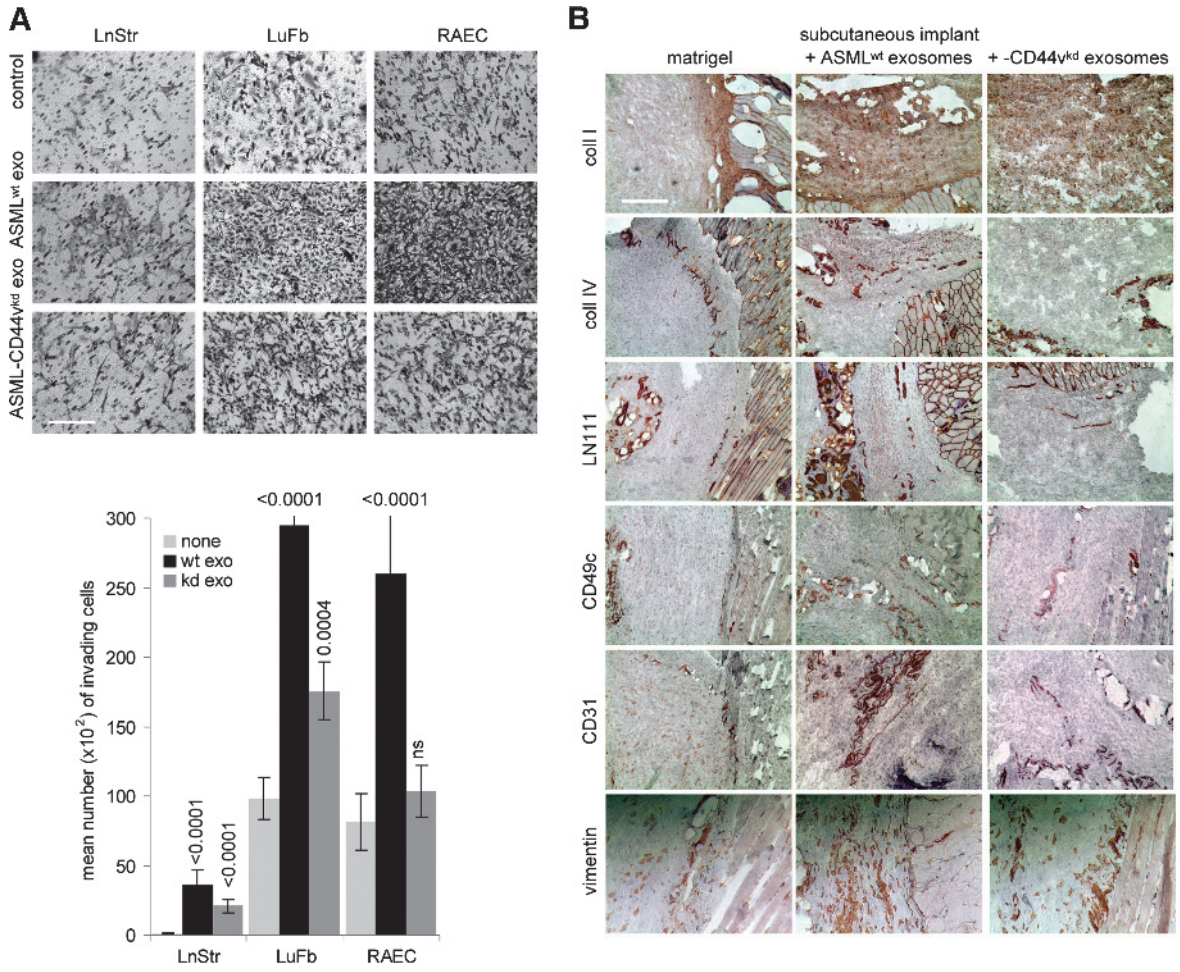

Figure 4. TEX-modulated CM promotes invasiveness. (A) Matrigel was mixed (1:1) with RPMI 1640 or TEX and was seeded on the lower membrane site of a transwell insert. LuFb, LnStr, and RAEC (5×10^4) were layered on the upper site of the insert. Matrigel immigration was evaluated after 24 hours. Representative examples (scale bar, 200 μm) and mean numbers (triplicates) ± SD of matrigel invading cells are shown. Significant differences between matrigel and TEX-pretreated matrigel are indicated by asterisk. (B) Matrigel was mixed (1:1) with PBS, which contained ASML^{wt} or ASML-CD44v^{kd} exosomes, as indicated. Matrigel was incubated for 12 hours at 37°C and was thereafter s.c. injected. The plug was removed after 5 days and was shock frozen. Plug sections were stained with anti–coll I, anti–coll IV, anti-LNγ1, anti-CD49c, anti-CD31, or anti-vimentin and were counterstained with H&E. Representative examples of the matrigel plug adjacent to host tissue are shown (scale bar, 200 μm). The exosome-modulated stroma matrix facilitates invasiveness.

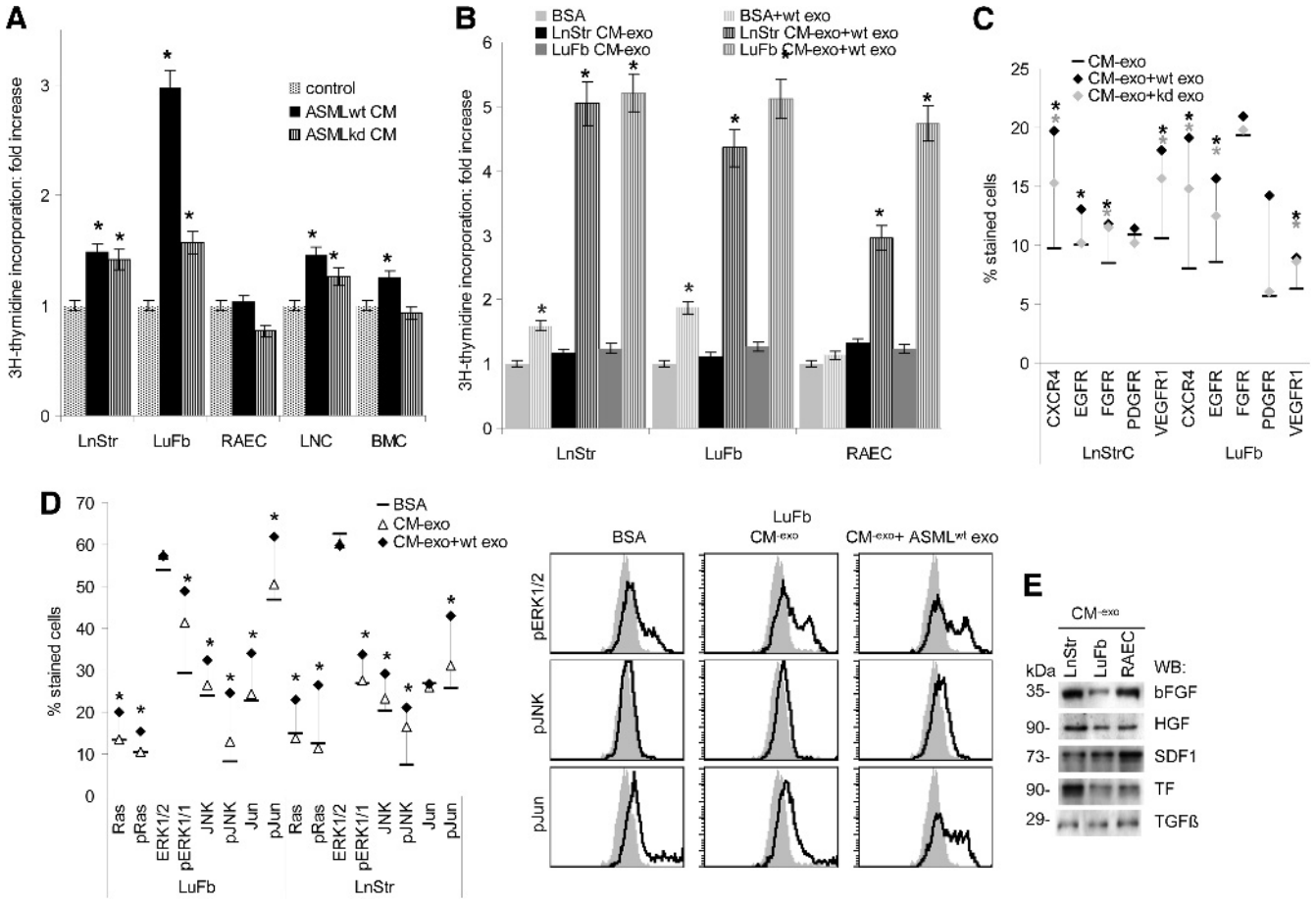

Figure 5. TEX-modulated CM promotes hematopoietic and stroma cell proliferation. (A and B) Cells were incubated with CM, CM^{-exo}, or TEX-pretreated CM^{-exo}, where TEX were removed by centrifugation. Proliferative activity was evaluated by ^{3}H-thymidine incorporation after 3 days of culture. (C) Flow cytometry analysis of LnStr and LuFb that were treated o/n with CM^{-exo} with or without $ASML^{wt}$ or ASML-$CD44v^{kd}$ exosomes. Mean values (three assays) of stained cells are shown. (D) LnStr and LuFb were incubated o/n with CM^{-exo} or $ASML^{wt}$ exosome–pretreated CM^{-exo}, where TEX were removed by centrifugation. LnStr and LuFb were stained with the indicated antibodies, evaluating protein expression by flow cytometry. Representative examples and mean values (triplicates) are shown. (A–D) Significant differences between CM^{-exo} and TEX-pretreated CM^{-exo} are indicated by asterisk. (E) Evaluation of cytokines and chemokines in LnStr, LuFb, and RAEC CM^{-exo} by WB. Growth promotion by TEX-treated LnStr and LuFb CM is accompanied by pronounced activation of the MAPK and JNK pathways and could be initiated by the liberation of growth factors from the CM by TEX, the LnStr, LuFb, and RAEC CM being rich in bFGF, HGF, SDF1, and TF.

was stronger when the CM was treated with $ASML^{wt}$ than ASML-$CD44v^{kd}$ exosomes (Figure 5*C*). Flow cytometry revealed pronounced extracellular signal-regulated kinase 1/2(ERK1/2), Jun kinase (JNK), and c-jun activation upon co-culture of LnStr and LuFb with their own CM^{-exo} that had been modulated by $ASML^{wt}$ exosomes (Figure 5*D*), which could be due to forced liberation/accessibility of matrix-deposited growth factors, LnStr, LuFb, and RAEC CM^{-exo} containing basic FGF (bFGF), hepatocyte growth factor (HGF), stroma derived factor 1 (SDF1), tissue factor (TF), and transforming growth factor β, bFGF being most abundantly recovered in LuFb and RAEC CM^{-exo} (Figures W4 and 5*E*).

TEX in concert with the tumor matrix can protect tumor cells from apoptosis [39,43]. $ASML^{wt}$ CM exerted a slight apoptosis-protective effect on LnStr, LuFb, and RAEC, though not on hematopoietic cells. The ASML-$CD44v^{kd}$ CM exerted no protective effect (Figure 6*A*). Exosome modulation of the matrix accounted for the protective effect, as it was also seen when the LnStr or the LuFb matrix was pretreated with $ASML^{wt}$ exosomes (Figure 6*B*). The underlying mechanism has not yet been elucidated. However, there is evidence that the TEX-modulated host matrix delivers signals promoting activation of the phosphatidylinositol 3-kinase (PI3K)/Akt pathway with pronounced BAD phosphorylation and recovery of Bcl2 and BclXl even in cisplatin-treated LnStr and LuFb, whereas recovery of Bax and Bak, cleaved caspase-9, and activated caspase-3 was slightly reduced (Figure 6*C*).

Taken together, TEX modulate the host matrix such that it strengthens stroma cell proliferation and drug resistance.

Discussion

As outlined by Hanahan and Weinberg [1], one important factor in tumor biology relies on the capacity of tumor cells to create a microenvironment by recruiting and modulating non-transformed cells that favor tumor cell survival and spreading/propagation [44–46]. Though the tumor-host talk is a conditio sine qua non for tumor development and progression, the intensity of this tumor host communication may vary, where tumors particularly prone for interacting with the host, like the most deadly PaCa, which are characterized by desmoplasia, severe paraneoplastic syndromes, and early metastatic spread, are burdened with poor prognosis [47–50]. With the current state of knowledge

not yet allowing an orchestrated view on the tumor-host cross talk, there is evidence that TEX are of central importance.

Exosomes are important intercellular communicators [14,20,51] that are abundantly delivered by tumor cells [52]. Exosomes are known to constitutively express tetraspanins and adhesion molecules [14], which contribute to exosome-selective target cell binding [23,53]. Exosomes also express proteases [28–31] that can modulate the exosome and target cell protein profiles [31–34]. Exosome binding can induce target cell activation, and through the transfer of mRNA and miRNA, exosomes contribute to target cell modulation [18–21]. These exosome activities will be of importance in the cross talk between cancer stem cell exosomes and neighboring cancer cells, the subject being heavily discussed but still awaiting a clear answer [54]; TEX are equally important for the cross talk between tumor cells and surrounding as well as distant stroma cells and hematopoietic progenitors. We and other groups provided evidence that stroma cells in the niche are direct targets for TEX and that the impact of TEX reaches beyond activation toward reprogramming [28,55,56]. In concern of hematopoietic progenitors, the paper by Peinado et al. [57] provided a proof on the central importance of TEX, the precise mechanism remaining to be explored. Furthermore, there is strong evidence that TEX also support recruitment of mesenchymal stem cell, which contributes to shaping the tumor microenvironment [58–60]. Besides this intercellular communication, TEX apparently also affect ECM components that we approached for the first time in the present manuscript. We became aware of the phenomenon noting that the CM of the highly metastatic ASML cells supports exosomes in premetastatic niche preparation, whereas CM from the poorly metastatic ASML-CD44v^{kd} cells does not [37]. On the basis of this finding, we asked whether TEX also affect the host cell matrix and whether host cell matrix modulation by TEX affects host cells. We describe that TEX degrade the host matrix, which strongly supports host cell migration and invasiveness as well as host

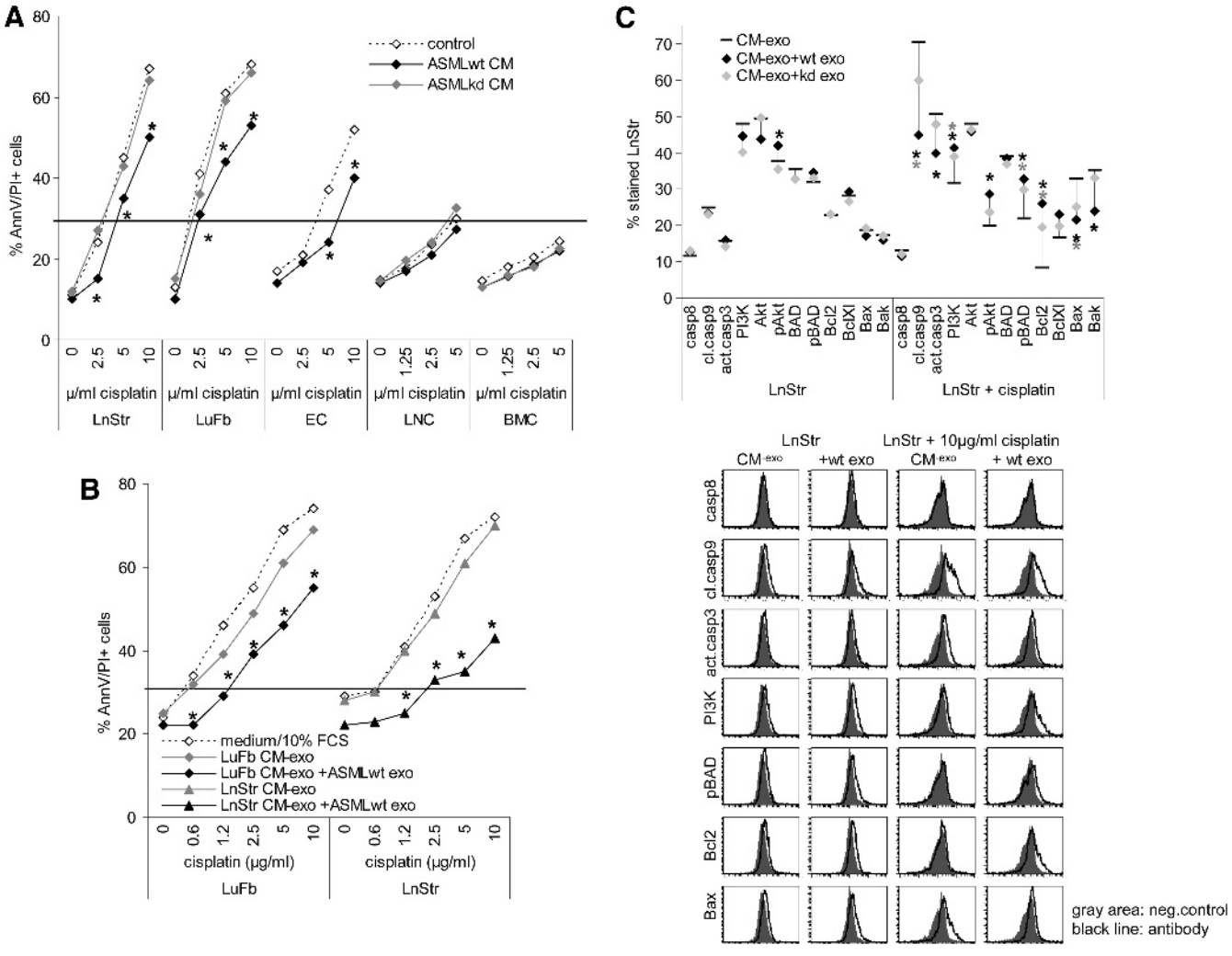

Figure 6. TEX-modulated CM promotes stroma cell drug resistance. (A and B) Cells were incubated with ASML CM or TEX-pretreated CM^{-exo}, removing TEX by centrifugation. Apoptosis resistance was evaluated by annexin V/propidium iodide (AnnV/PI) staining after 3 days of culture in the presence of titrated amounts of cisplatin. Mean values (triplicates) are shown. (C) Cells were incubated for 24 hours with CM^{-exo} or TEX-pretreated CM^{-exo}, where indicated cultures contained 10 μg/ml cisplatin. Cells were fixed and permeabilized, and expression of the indicated apoptosis/anti-apoptosis markers was evaluated by flow cytometry. Representative examples and mean values (three assays) are shown. (A–C) Significant differences between CM^{-exo} and TEX-pretreated CM^{-exo} are indicated by asterisk. Modulation of the stroma matrix by TEX promotes drug resistance of stroma cells, initiated by pronounced activation of the PI3K/Akt pathway.

cell proliferation and apoptosis resistance. Thus, the impact of TEX on the host matrix can have severe consequences on tumor progression.

TEX Binding to the Host Matrix

TEX bind to selective components of the ECM, and selectivity of binding is determined by the adhesion molecule profile of the exosomes. Thus, ASML^{wt} bind more efficiently than ASML-CD44v^{kd} exosomes to coll I, II, III, and IV as well as to FN and, particularly HA, whereas both exosomes bind equally well to LN111, LN332, and VN. Antibody blocking studies revealed that coll binding proceeds predominantly through α_3, LN binding through α_3 and $\alpha_6\beta_4$, and HA binding through CD44, where the lower efficacy of ASML-CD44v^{kd} binding could rely on reduced $\alpha_6\beta_4$ and CD44 expression [39]. In addition, ASML-CD44v^{kd}, distinct to ASML^{wt} CM, mostly contains low molecular weight HA [39], which could explain the poor adhesion of ASML^{wt} and ASML-CD44v^{kd} exosomes to the ASML-CD44v^{kd} CM. Not performing a detailed pulldown proteome analysis, we cannot exclude a contribution of additional exosomal adhesion molecules. It is, however, important to note that TEX do not only bind to purified matrix proteins but equally well or with higher affinity to host stroma *in vitro* as well as *in vivo*, where ASML^{wt} exosomes are abundantly recovered in the ECM of muscles, the submucosa of the gastrointestinal tract, the perivascular region, and the basal lamina of several organs like skin and tongue. With these matrices being composed of several matrix proteins, a clear assignment of TEX binding to individual components was not possible, but coll and LNs apparently are preferred targets.

A first hint toward biologic significance of TEX binding selective tissue matrices was the finding that ASML cells, in all instances and with high preference metastasizing through lymph nodes to the lungs, occasionally grow along tissue matrices that abundantly bind ASML-TEX, like muscle and skin, without invading or destructing the adjacent tissue.

Thus, TEX bind through adhesion molecules to selective matrix components, the reduced $\alpha_6\beta_4$ and CD44 expression in ASML-CD44v^{kd} exosomes obviously accounting for the impaired cross talk with the ECM. There is evidence that host matrix modulation by TEX favors tumor cell attraction and/or motility/invasiveness.

ECM Modulation by TEX

With ECM binding supporting metastasizing tumor cell invasion, the question arose on matrix modulation by TEX. Exosome binding severely affects the host matrix, the most dominant feature being matrix degradation. Exosomes abundantly contain matrix-degrading enzymes [14]. In ASML^{wt} exosomes, particularly high level of uPAR, MMP2, MMP3, MMP9, MMP14, and ADAM17 are recovered. Corresponding to the recovery in ASML-CD44v^{kd} cells, uPAR, MMP9, MMP13, and ADAM17 are reduced in ASML-CD44v^{kd} exosomes. As demonstrated for gelatin degradation and by WB for several coll, FN, LN111, and LN332, exosomal proteases are function-competent [28–30], which also account for the degradation of the ECM of stroma lines and endothelial cells (EC).

Taken together, besides adhesion molecules, exosomal proteases are essential for the cross talk between a tumor and the host matrix by creating space, possibly by contributing to matrix protein maturation as described for the ADAMTS family that contributes to procollagen maturation [61,62] as well as by generating fragments of matrix proteins that exert distinct functions like the motility promoting LN332 fragment [63] or the small HA fragments that promote an inflammatory milieu [64]. Indeed, modulation of the host ECM by TEX has severe consequences for the host cells.

TEX-Modulated Host Matrix and Stroma Cell Adhesion, Migration, and Invasion

The TEX-modulated host cell matrix promotes host cell adhesion and, more pronounced, host cell motility and invasiveness.

LnStr, LuFb, and RAEC adhere more efficiently to their own matrix than to plastic. Adhesion becomes further facilitated when the host matrix is modulated by TEX, which accounts particularly for LuFb and RAEC, ASML^{wt} exosomes exerting a stronger effect than ASML-CD44v^{kd} exosomes. Spriting of the cells is more pronounced on CM than on plastic. Spriting is not significantly altered by exosome modulation of the CM. Instead, there is evidence for a more pronounced formation of focal adhesion clusters, which can contribute to cell motility [65], the latter being strikingly affected by TEX, as revealed by transwell migration, time lapse video microscopy, and *in vitro* wound healing. Of particular importance, TEX facilitate invasiveness as shown *in vitro* for matrigel penetration and confirmed *in vivo*, where particularly EC but also fibroblast invade with far higher efficiency an ASML^{wt} exosome–modulated than an untreated matrigel plug. In line with the lower efficacy of ASML-CD44v^{kd} exosomes in CM degradation, host cell motility and invasiveness were less or minimally affected by ASML-CD44v^{kd} exosome–modulated CM or matrigel.

We showed recently that ASML^{wt} CM facilitates recruitment of tumor cells into the draining lymph node [37]. It is also known that metastasizing tumors facilitate the recruitment of BMC into the premetastatic niche [57,66–68], TEX being speculated to fulfill this task [57]. Furthermore, TEX are suggested to promote angiogenesis [6,69–72]. Our data strongly support these hypotheses and provide for the first time evidence that host cell migration may not be exclusively a consequence of a direct interaction between host cells and TEX. Instead, the TEX-modulated host matrix will facilitate host cell migration, most strikingly demonstrated for the *in vivo* recruitment of EC and fibroblasts into a TEX-modulated matrigel plug. These findings expand the activity range of TEX and can explain the hitherto difficult to understand phenomenon of, e.g., hematopoietic progenitor recruitment toward the premetastatic organs rather than toward the primary tumor.

The TEX-Modulated Host Matrix Promotes Stroma Cell Activation

TEX severely affect host cells [20,54]. This can be initiated by exosome binding [73,74] or the transfer of exosomal mRNA and miRNA [18,75–78]. Thus, the work by Peinado et al. suggests the direct transfer of c-Met [57]. Our own work demonstrated that the uptake of TEX is accompanied by up-regulation of follstatin, MDR1, PLA2, and SSP1, to name only a few proteins whose expression promotes stroma cell survival. In addition, apoptosis regulating miR 24-1 is abundant in ASML TEX and is transferred into stroma cells [21]. We now present evidence that in a feedback the TEX-modulated host matrix also affects, though to a minor degree, host cell proliferation and apoptosis. These features fit well to the described feedback of the tumor matrix on tumor cells, which for the ASML^{wt} CM was shown to promote through CD44v6 the activation of c-Met and the $\alpha_6\beta_4$ integrin [39]. Growth promotion by the TEX-modulated host matrix may proceed through distinct pathways, as we noted significant up-regulation of the EGFR and, only by ASML^{wt} exosomes, the PDGFR in LuFb. Stimulation of the EGFR as well as of the FGFR could proceed through binding of their ligands [79–81], liberated from the CM by ASML exosomes. In

this respect, it should be mentioned that growth factor bioavailability depends on the ECM stiffness [82,83]. Thus, matrix protein degradation by TEX could well account for a feedback from the stroma matrix toward the stroma cell through easier access to matrix-integrated growth factors and chemokines. Stimulation of stroma cells could be further supported by binding of TEX-modulated matrix proteins, coll and LN fragments being known to display growth factor activity [82,84].

Both EGFR and FGFR whose expression became upregulated when cultured in the presence of the TEX-modulated stroma matrix are known to activate the Ras/Raf/mitogen-activated protein kinase (MAPK) and PI3K/Akt pathways [79,85–88]. Pronounced ERK1/2, JNK, and c-jun phosphorylation after culturing stroma cells in the presence of the TEX-modulated matrix could thus account for pronounced proliferation. Our data also suggest that higher apoptosis resistance relies on EGFR and PDGFR up-regulation, as PI3K, Akt, and Bad phosphorylation was pronounced and Bcl2 expression was upregulated, whereas caspase-8 expression was unaltered, but caspase-9 cleavage was reduced and caspase-3 was less efficiently activated in cultures containing TEX-modulated matrix, indicating stimulation of apoptosis protection rather than down-regulation of receptor-mediated apoptosis.

Taken together, TEX binding and uptake stimulate and reprogram stroma cells allowing for phenotypic changes, proliferation, and apoptosis resistance, which, besides metastatic organs, will in the first instance affect the primary tumor's environment, where the TEX-modulated host matrix in a feedback loop contributes to host cell proliferation and apoptosis resistance. This may particularly account for PaCa, the high level of CD44v6, and $\alpha_6\beta_4$ expression on PaCa TEX, favoring an intense cross talk with the pancreatic tissue stroma and allowing the directly or indirectly associated proteases like MMP14 and TACE and MMP3, MMP7, and MMP9 to generate a milieu that favors recruitment of endothelial cell progenitors [89,90] as well as of stimulation of resident fibroblasts toward myofibroblast [91,92].

Conclusion

Taken together, TEX bind matrix proteins and exosomal proteases modulate the matrix, which facilitates motility, creates space for migrating tumor as well as host cells, and attracts tumor cells, stroma cells, and inflammatory cells by degraded matrix proteins and likely the liberation of chemokines and growth factors.

It is well appreciated that TEX binding to and uptake by target cells severely affects the target cell fate. We here demonstrate that modulation of the matrix by TEX should not be neglected as it adds to host cell modulation, particularly motility, recruitment, and invasiveness. These features unlikely are restricted to TEX; instead, exosome-mediated matrix modulation could well be important in organogenesis including vasculogenesis, wound healing, and coagulation.

Acknowledgments

We thank Christine Niesik and Angela Frank for help with animal experiments, flow cytometry, immunohistology, and exosome preparation.

References

[1] Hanahan D and Weinberg RA (2011). Hallmarks of cancer: the next generation. *Cell* **144**, 646–674.
[2] Hanahan D and Folkman J (1996). Patterns and emerging mechanisms of the angiogenic switch during tumorigenesis. *Cell* **86**, 353–364.
[3] Stewart TJ and Smyth MJ (2011). Improving cancer immunotherapy by targeting tumor-induced immune suppression. *Cancer Metastasis Rev* **30**, 125–140.
[4] Brabletz T (2012). EMT and MET in metastasis: where are the cancer stem cells? *Cancer Cell* **22**, 699–701.
[5] Kaplan RN, Rafii S, and Lyden D (2006). Preparing the "soil": the premetastatic niche. *Cancer Res* **66**, 11089–11093.
[6] Bussolati B, Grange C, and Camussi G (2011). Tumor exploits alternative strategies to achieve vascularization. *FASEB J* **25**, 2874–2882.
[7] Taylor DD and Gercel-Taylor C (2011). Exosomes/microvesicles: mediators of cancer-associated immunosuppressive microenvironments. *Semin Immunopathol* **33**, 441–454.
[8] Garnier D, Magnus N, Lee TH, Bentley V, Meehan B, Milsom C, Montermini L, Kislinger T, and Rak J (2012). Cancer cells induced to express mesenchymal phenotype release exosome–like extracellular vesicles carrying tissue factor. *J Biol Chem* **287**, 43565–43572.
[9] Alderton GK (2012). Metastasis. Exosomes drive premetastatic niche formation. *Nat Rev Cancer* **12**, 447.
[10] Pap E, Pállinger E, Pásztói M, and Falus A (2009). Highlights of a new type of intercellular communication: microvesicle-based information transfer. *Inflamm Res* **58**, 1–8.
[11] Denzer K, Kleijmeer MJ, Heijnen HF, Stoorvogel W, and Geuze HJ (2000). Exosome: from internal vesicle of the multivesicular body to intercellular signaling device. *J Cell Sci* **113**, 3365–3374.
[12] van Niel G, Porto-Carreiro I, Simoes S, and Raposo G (2006). Exosomes: a common pathway for a specialized function. *J Biochem* **140**, 13–21.
[13] Lakkaraju A and Rodriguez-Boulan E (2008). Itinerant exosomes: emerging roles in cell and tissue polarity. *Trends Cell Biol* **18**, 199–209.
[14] Mathivanan S, Ji H, and Simpson RJ (2010). Exosomes: extracellular organelles important in intercellular communication. *J Proteomics* **73**, 1907–1920.
[15] Rak J (2010). Microparticles in cancer. *Semin Thromb Hemost* **36**, 888–906.
[16] Raimondo F, Morosi L, Chinello C, Magni F, and Pitto M (2011). Advances in membranous vesicle and exosome proteomics improving biological understanding and biomarker discovery. *Proteomics* **11**, 709–720.
[17] Zöller M (2009). Tetraspanins: push and pull in suppressing and promoting metastasis. *Nat Rev Cancer* **9**, 40–55.
[18] Valadi H, Ekström K, Bossios A, Sjöstrand M, Lee JJ, and Lötvall JO (2007). Exosome-mediated transfer of mRNAs and microRNAs is a novel mechanism of genetic exchange between cells. *Nat Cell Biol* **9**, 654–659.
[19] Chen X, Liang H, Zhang J, Zen K, and Zhang CY (2012). Horizontal transfer of microRNAs: molecular mechanisms and clinical applications. *Protein Cell* **3**, 28–37.
[20] Kharaziha P, Ceder S, Li Q, and Panaretakis T (2012). Tumor cell-derived exosomes: a message in a bottle. *Biochim Biophys Acta* **1826**, 103–111.
[21] Rana S, Malinowska K, and Zöller M (2013). Exosomal tumor microRNA modulates premetastatic organ cells. *Neoplasia* **15**, 281–295.
[22] Tian T, Zhu YL, Hu FH, Wang YY, Huang NP, and Xiao ZD (2012). Dynamics of exosome internalization and trafficking. *J Cell Physiol* **228**, 1487–1495.
[23] Rana S, Yue S, Stadel D, and Zöller M (2012). Toward tailored exosomes: the exosomal tetraspanin web contributes to target cell selection. *Int J Biochem Cell Biol* **44**, 1574–1584.
[24] Chaput N, Flament C, Viaud S, Taieb J, Roux S, Spatz A, André F, LePecq JB, Boussac M, Garin J, et al. (2006). Dendritic cell derived-exosomes: biology and clinical implementations. *J Leukoc Biol* **80**, 471–478.
[25] Viaud S, Ploix S, Lapierre V, Théry C, Commere PH, Tramalloni D, Gorrichon K, Virault-Rocroy P, Tursz T, Lantz O, et al. (2011). Updated technology to produce highly immunogenic dendritic cell-derived exosomes of clinical grade: a critical role of interferon-γ. *J Immunother* **34**, 65–75.
[26] Xie Y, Bai O, Zhang H, Yuan J, Zong S, Chibbar R, Slattery K, Qureshi M, Wei Y, Deng Y, et al. (2010). Membrane-bound HSP70-engineered myeloma cell-derived exosomes stimulate more efficient $CD8^+$ CTL- and NK-mediated antitumour immunity than exosomes released from heat-shocked tumour cells expressing cytoplasmic HSP70. *J Cell Mol Med* **14**, 2655–2666.
[27] van Noort JM, Bsibsi M, Nacken P, Gerritsen WH, and Amor S (2012). The link between small heat shock proteins and the immune system. *Int J Biochem Cell Biol* **44**, 1670–1679.
[28] Lee TH, D'Asti E, Magnus N, Al-Nedawi K, Meehan B, and Rak J (2011). Microvesicles as mediators of intercellular communication in cancer—the emerging science of cellular 'debris'. *Semin Immunopathol* **33**, 455–467.
[29] Escrevente C, Morais VA, Keller S, Soares CM, Altevogt P, and Costa J (2008). Functional role of *N*-glycosylation from ADAM10 in processing, localization and activity of the enzyme. *Biochim Biophys Acta* **1780**, 905–913.

[30] Hakulinen J, Sankkila L, Sugiyama N, Lehti K, and Keski-Oja J (2008). Secretion of active membrane type 1 matrix metalloproteinase (MMP-14) into extracellular space in microvesicular exosomes. *J Cell Biochem* **105**, 1211–1218.

[31] Ngora H, Galli UM, Miyazaki K, and Zöller M (2012). Membrane-bound and exosomal metastasis-associated C4.4A promotes migration by associating with the $\alpha_6\beta_4$ integrin and MT1-MMP. *Neoplasia* **14**, 95–107.

[32] Stoeck A, Keller S, Riedle S, Sanderson MP, Runz S, Le Naour F, Gutwein P, Ludwig A, Rubinstein E, and Altevogt P (2006). A role for exosomes in the constitutive and stimulus-induced ectodomain cleavage of L1 and CD44. *Biochem J* **393**, 609–618.

[33] Qu Y, Franchi L, Nunez G, and Dubyak GR (2007). Nonclassical IL-1β secretion stimulated by P2X7 receptors is dependent on inflammasome activation and correlated with exosome release in murine macrophages. *J Immunol* **179**, 1913–1925.

[34] Sanderson MP, Keller S, Alonso A, Riedle S, Dempsey PJ, and Altevogt P (2008). Generation of novel, secreted epidermal growth factor receptor (EGFR/ErbB1) isoforms via metalloprotease-dependent ectodomain shedding and exosome secretion. *J Cell Biochem* **103**, 1783–1797.

[35] Matzku S, Komitowski D, Mildenberger M, and Zöller M (1983). Characterization of BSp73, a spontaneous rat tumor and its *in vivo* selected variants showing different metastasizing capacities. *Invasion Metastasis* **3**, 109–123.

[36] Klingbeil P, Marhaba R, Jung T, Kirmse R, Ludwig T, and Zöller M (2009). CD44 variant isoforms promote metastasis formation by a tumor cell-matrix cross-talk that supports adhesion and apoptosis resistance. *Mol Cancer Res* **7**, 168–179.

[37] Jung T, Castellana D, Klingbeil P, Cuesta Hernández I, Vitacolonna M, Orlicky DJ, Roffler SR, Brodt P, and Zöller M (2009). CD44v6 dependence of premetastatic niche preparation by exosomes. *Neoplasia* **11**, 1093–1105.

[38] LeBedis C, Chen K, Fallavollita L, Boutros T, and Brodt P (2002). Peripheral lymph node stromal cells can promote growth and tumorigenicity of breast carcinoma cells through the release of IGF-I and EGF. *Int J Cancer* **100**, 2–8.

[39] Jung T, Gross W, and Zöller M (2011). CD44v6 coordinates tumor matrix-triggered motility and apoptosis resistance. *J Biol Chem* **286**, 15862–15874.

[40] Kopfstein L and Christofori G (2006). Metastasis: cell-autonomous mechanisms versus contributions by the tumor microenvironment. *Cell Mol Life Sci* **63**, 449–468.

[41] Epifano C and Perez-Moreno M (2012). Crossroads of integrins and cadherins in epithelia and stroma remodeling. *Cell Adh Migr* **6**, 261–273.

[42] Castells M, Thibault B, Delord JP, and Couderc B (2012). Implication of tumor microenvironment in chemoresistance: tumor-associated stromal cells protect tumor cells from cell death. *Int J Mol Sci* **13**, 9545–9571.

[43] Cai Z, Yang F, Yu L, Yu Z, Jiang L, Wang Q, Yang Y, Wang L, Cao X, and Wang J (2012). Activated T cell exosomes promote tumor invasion via Fas signaling pathway. *J Immunol* **188**, 5954–5961.

[44] Mareel MM, Van Roy FM, and Bracke ME (1993). How and when do tumor cells metastasize? *Crit Rev Oncog* **4**, 559–594.

[45] Sleeman JP, Christofori G, Fodde R, Collard JG, Berx G, Decraene C, and Rüegg C (2012). Concepts of metastasis in flux: the stromal progression model. *Semin Cancer Biol* **22**, 174–186.

[46] Nakasone ES, Askautrud HA, Kees T, Park JH, Plaks V, Ewald AJ, Fein M, Rasch MG, Tan YX, Qiu J, et al. (2012). Imaging tumor-stroma interactions during chemotherapy reveals contributions of the microenvironment to resistance. *Cancer Cell* **21**, 488–503.

[47] Erkan M, Hausmann S, Michalski CW, Fingerle AA, Dobritz M, Kleeff J, and Friess H (2012). The role of stroma in pancreatic cancer: diagnostic and therapeutic implications. *Nat Rev Gastroenterol Hepatol* **9**, 454–467.

[48] Dumitrascu DL, Suciu O, Grad C, and Gheban D (2010). Thrombotic complications of pancreatic cancer: classical knowledge revisited. *Dig Dis* **28**, 350–354.

[49] Karamitopoulou E (2012). Tumor budding cells, cancer stem cells and epithelial-mesenchymal transition-type cells in pancreatic cancer. *Front Oncol* **2**, 209.

[50] Abel EV and Simeone DM (2013). Biology and clinical applications of pancreatic cancer stem cells. *Gastroenterology* **144**, 1241–1248.

[51] Ge R, Tan E, Sharghi-Namini S, and Asada HH (2012). Exosomes in cancer microenvironment and beyond: have we overlooked these extracellular messengers? *Cancer Microenviron* **5**, 323–332.

[52] Vlassov AV, Magdaleno S, Setterquist R, and Conrad R (2012). Exosomes: current knowledge of their composition, biological functions, and diagnostic and therapeutic potentials. *Biochim Biophys Acta* **1820**, 940–948.

[53] Rana S and Zöller M (2011). Exosome target cell selection and the importance of exosomal tetraspanins: a hypothesis. *Biochem Soc Trans* **39**, 559–562.

[54] Quesenberry PJ and Aliotta JM (2010). Cellular phenotype switching and microvesicles. *Adv Drug Deliv Rev* **62**, 1141–1148.

[55] Martins VR, Dias MS, and Hainaut P (2013). Tumor-cell-derived microvesicles as carriers of molecular information in cancer. *Curr Opin Oncol* **25**, 66–75.

[56] Peinado H, Lavotshkin S, and Lyden D (2011). The secreted factors responsible for pre-metastatic niche formation: old sayings and new thoughts. *Semin Cancer Biol* **21**, 139–146.

[57] Peinado H, Aleèkoviæ M, Lavotshkin S, Matei I, Costa-Silva B, Moreno-Bueno G, Hergueta-Redondo M, Williams C, García-Santos G, Ghajar C, et al. (2012). Melanoma exosomes educate bone marrow progenitor cells toward a pro-metastatic phenotype through MET. *Nat Med* **18**, 883–891.

[58] Cho JA, Park H, Lim EH, and Lee KW (2012). Exosomes from breast cancer cells can convert adipose tissue-derived mesenchymal stem cells into myofibroblast-like cells. *Int J Oncol* **40**, 130–138.

[59] Gu J, Qian H, Shen L, Zhang X, Zhu W, Huang L, Yan Y, Mao F, Zhao C, Shi Y, et al. (2012). Gastric cancer exosomes trigger differentiation of umbilical cord derived mesenchymal stem cells to carcinoma-associated fibroblasts through TGF-β/Smad pathway. *PLoS One* **7**, e52465.

[60] Zhu W, Huang L, Li Y, Zhang X, Gu J, Yan Y, Xu X, Wang M, Qian H, and Xu W (2012). Exosomes derived from human bone marrow mesenchymal stem cells promote tumor growth *in vivo*. *Cancer Lett* **315**, 28–37.

[61] Colige A, Ruggiero F, Vandenberghe I, Dubail J, Kesteloot F, Van Beeumen J, Beschin A, Brys L, Lapière CM, and Nusgens B (2005). Domains and maturation processes that regulate the activity of ADAMTS-2, a metalloproteinase cleaving the aminopropeptide of fibrillar procollagens types I–III and V. *J Biol Chem* **280**, 34397–34408.

[62] Apte SS (2009). A disintegrin-like and metalloprotease (reprolysin-type) with thrombospondin type 1 motif (ADAMTS) superfamily: functions and mechanisms. *J Biol Chem* **284**, 31493–31497.

[63] Malinda KM, Wysocki AB, Koblinski JE, Kleinman HK, and Ponce ML (2008). Angiogenic laminin-derived peptides stimulate wound healing. *Int J Biochem Cell Biol* **40**, 2771–2780.

[64] Cantor JO and Nadkarni PP (2006). Hyaluronan: the Jekyll and Hyde molecule. *Inflamm Allergy Drug Targets* **5**, 257–260.

[65] McNiven MA, Baldassarre M, and Buccione R (2004). The role of dynamin in the assembly and function of podosomes and invadopodia. *Front Biosci* **9**, 1944–1953.

[66] Erler JT, Bennewith KL, Cox TR, Lang G, Bird D, Koong A, Le QT, and Giaccia AJ (2009). Hypoxia-induced lysyl oxidase is a critical mediator of bone marrow cell recruitment to form the premetastatic niche. *Cancer Cell* **15**, 35–44.

[67] Gil-Bernabé AM, Ferjancic S, Tlalka M, Zhao L, Allen PD, Im JH, Watson K, Hill SA, Amirkhosravi A, Francis JL, et al. (2012). Recruitment of monocytes/macrophages by tissue factor-mediated coagulation is essential for metastatic cell survival and premetastatic niche establishment in mice. *Blood* **119**, 3164–3175.

[68] Sceneay J, Chow MT, Chen A, Halse HM, Wong CS, Andrews DM, Sloan EK, Parker BS, Bowtell DD, Smyth MJ, et al. (2012). Primary tumor hypoxia recruits $CD11b^+/Ly6C^{med}/Ly6G^+$ immune suppressor cells and compromises NK cell cytotoxicity in the premetastatic niche. *Cancer Res* **72**, 3906–3911.

[69] Gesierich S, Berezovskiy I, Ryschich E, and Zöller M (2006). Systemic induction of the angiogenesis switch by the tetraspanin D6.1A/CO-029. *Cancer Res* **66**, 7083–7094.

[70] Park JE, Tan HS, Datta A, Lai RC, Zhang H, Meng W, Lim SK, and Sze SK (2010). Hypoxic tumor cell modulates its microenvironment to enhance angiogenic and metastatic potential by secretion of proteins and exosomes. *Mol Cell Proteomics* **9**, 1085–1099.

[71] Nazarenko I, Rana S, Baumann A, McAlear J, Hellwig A, Trendelenburg M, Lochnit G, Preissner KT, and Zöller M (2010). Cell surface tetraspanin Tspan8 contributes to molecular pathways of exosome-induced endothelial cell activation. *Cancer Res* **70**, 1668–1678.

[72] Sheldon H, Heikamp E, Turley H, Dragovic R, Thomas P, Oon CE, Leek R, Edelmann M, Kessler B, Sainson RC, et al. (2010). New mechanism for Notch signaling to endothelium at a distance by Delta-like 4 incorporation into exosomes. *Blood* **116**, 2385–2394.

[73] Bu N, Wu H, Sun B, Zhang G, Zhan S, Zhang R, and Zhou L (2011). Exosome-loaded dendritic cells elicit tumor-specific $CD8^+$ cytotoxic T cells in patients with glioma. *J Neurooncol* **104**, 659–667.

[74] Yang M, Li Y, Chilukuri K, Brady OA, Boulos MI, Kappes JC, and Galileo DS (2011). L1 stimulation of human glioma cell motility correlates with FAK activation. *J Neurooncol* **105**, 27–44.

[75] Mittelbrunn M, Gutiérrez-Vázquez C, Villarroya-Beltri C, González S, Sánchez-Cabo F, González MÁ, Bernad A, and Sánchez-Madrid F (2011). Unidirectional transfer of microRNA-loaded exosomes from T cells to antigen-presenting cells. *Nat Commun* **2**, 282.

[76] Montecalvo A, Larregina AT, Shufesky WJ, Stolz DB, Sullivan ML, Karlsson JM, Baty CJ, Gibson GA, Erdos G, Wang Z, et al. (2012). Mechanism of transfer of functional microRNAs between mouse dendritic cells via exosomes. *Blood* **119**, 756–766.

[77] Xin H, Li Y, Buller B, Katakowski M, Zhang Y, Wang X, Shang X, Zhang ZG, and Chopp M (2012). Exosome-mediated transfer of miR-133b from multipotent mesenchymal stromal cells to neural cells contributes to neurite outgrowth. *Stem Cells* **30**, 1556–1564.

[78] Umezu T, Ohyashiki K, Kuroda M, and Ohyashiki JH (in press). Leukemia cell to endothelial cell communication via exosomal miRNAs. *Oncogene*. DOI:10.1038/onc.2012.295, E-pub ahead of print.

[79] Han W and Lo HW (2012). Landscape of EGFR signaling network in human cancers: biology and therapeutic response in relation to receptor subcellular locations. *Cancer Lett* **318**, 124–134.

[80] Seshacharyulu P, Ponnusamy MP, Haridas D, Jain M, Ganti AK, and Batra SK (2012). Targeting the EGFR signaling pathway in cancer therapy. *Expert Opin Ther Targets* **16**, 15–31.

[81] Wesche J, Haglund K, and Haugsten EM (2011). Fibroblast growth factors and their receptors in cancer. *Biochem J* **437**, 199–213.

[82] Hynes RO (2009). The extracellular matrix: not just pretty fibrils. *Science* **326**, 1216–1219.

[83] Brizzi MF, Tarone G, and Defilippi P (2012). Extracellular matrix, integrins, and growth factors as tailors of the stem cell niche. *Curr Opin Cell Biol* **24**, 645–651.

[84] Panayotou G, End P, Aumailley M, Timpl R, and Engel J (1989). Domains of laminin with growth-factor activity. *Cell* **56**, 93–101.

[85] Lo HW (2010). EGFR-targeted therapy in malignant glioma: novel aspects and mechanisms of drug resistance. *Curr Mol Pharmacol* **3**, 37–52.

[86] Eccles SA (2011). The epidermal growth factor receptor/Erb-B/HER family in normal and malignant breast biology. *Int J Dev Biol* **55**, 685–696.

[87] Dey JH, Bianchi F, Voshol J, Bonenfant D, Oakeley EJ, and Hynes NE (2010). Targeting fibroblast growth factor receptors blocks PI3K/AKT signaling, induces apoptosis, and impairs mammary tumor outgrowth and metastasis. *Cancer Res* **70**, 4151–4162.

[88] Berg M and Soreide K (2012). EGFR and downstream genetic alterations in KRAS/BRAF and PI3K/AKT pathways in colorectal cancer: implications for targeted therapy. *Discov Med* **14**, 207–214.

[89] John A and Tuszynski G (2001). The role of matrix metalloproteinases in tumor angiogenesis and tumor metastasis. *Pathol Oncol Res* **7**, 14–23.

[90] van Hinsbergh VW and Koolwijk P (2008). Endothelial sprouting and angiogenesis: matrix metalloproteinases in the lead. *Cardiovasc Res* **78**, 203–212.

[91] Kim BG, An HJ, Kang S, Choi YP, Gao MQ, Park H, and Cho NH (2011). Laminin-332-rich tumor microenvironment for tumor invasion in the interface zone of breast cancer. *Am J Pathol* **178**, 373–381.

[92] Shields MA, Dangi-Garimella S, Redig AJ, and Munshi HG (2012). Biochemical role of the collagen-rich tumour microenvironment in pancreatic cancer progression. *Biochem J* **441**, 541–552.

Table W1. List of Antibodies.

Antibody	Supplier	Antibody	Supplier
$\alpha_6\beta_4$	Clone B5.5 [1]	Hyaluronan	Rockland, Gilbertsville, PA
Akt	BD, Heidelberg, Germany	HGF	Santa Cruz, Heidelberg, Germany
ADAM10	Santa Cruz, Heidelberg, Germany	HGDF	Santa Cruz, Heidelberg, Germany
ADAM17	Santa Cruz, Heidelberg, Germany	HAdase	Santa Cruz, Heidelberg, Germany
ADAMTS1	Santa Cruz, Heidelberg, Germany	LNγ1	Rockland, Gilbertsville, PA
ADAMTS5	Santa Cruz, Heidelberg, Germany	LNγ2	BD, Heidelberg, Germany
ADAMTS8	Santa Cruz, Heidelberg, Germany	MMP2	Dianova, Hamburg, Germany
BAD	Santa Cruz, Heidelberg, Germany	MMP3	Santa Cruz, Heidelberg, Germany
Bcl2	BD, Heidelberg, Germany	MMP9	Dianova, Hamburg, Germany
BclXl	BD, Heidelberg, Germany	MMP13	Dianova, Hamburg, Germany
bFGF	Oncogene, Boston, MA	MMP14	Santa Cruz, Heidelberg, Germany
act.Caspase3	BD, Heidelberg, Germany	Osteopontin	Santa Cruz, Heidelberg, Germany
Caspase8	BD, Heidelberg, Germany	p38	BD, Heidelberg, Germany
cl.Caspase9	BD, Heidelberg, Germany	p-Akt	BD, Heidelberg, Germany
CD11b	Clone Ox42 (EAACC)	p-BAD	Santa Cruz, Heidelberg, Germany
CD11c	Clone Ox41 (EAACC)	p-c-jun	BD, Heidelberg, Germany
CD13	[2]	PDGF	BD, Heidelberg, Germany
CD18	BD, Heidelberg, Germany	PDGFR	BD, Heidelberg, Germany
CD29	BD, Heidelberg, Germany	p-ERK1,2	BD, Heidelberg, Germany
CD31	BD, Heidelberg, Germany	PI3K	Santa Cruz, Heidelberg, Germany
CD44s	Clone Ox50 (EAACC)	p-JNK	BD, Heidelberg, Germany
CD44v6	Clone A2.6 [1]	p-p38	BD, Heidelberg, Germany
CD49b	BD, Heidelberg, Germany	p-ras	BD, Heidelberg, Germany
CD49c	BD, Heidelberg, Germany	ras	BD, Heidelberg, Germany
CD54	Biozol, Eching, Germany	SDF1	Abcam, Cambridge, United Kingdom
CD104	BD, Heidelberg, Germany	Tenascin	LabVision, Fremont, CA
Coll I	Rockland, Gilbertsville, PA	TF	Santa Cruz, Heidelberg, Germany
Coll II	LabVision, Fremont, CA	Transforming growth factor β	Santa Cruz, Heidelberg, Germany
Coll IV	Rockland, Gilbertsville, PA	uPA	Calbiochem, Darmstadt, Germany
CXCR4	Santa Cruz, Heidelberg, Germany	uPAR	Calbiochem, Darmstadt, Germany
EGFR	Santa Cruz, Heidelberg, Germany	VEGF	Biotrend, Köln, Germany
ERK1/2	BD, Heidelberg, Germany	VEGFR1	Biotrend, Köln, Germany
FGFR	Santa Cruz, Heidelberg, Germany	Vimentin	BD, Heidelberg, Germany
FN	BD, Heidelberg, Germany	Vitronectin	Biotrend, Köln, Germany
		vWF	Abcam, Cambridge, United Kingdom
mIgG, mIgG, rabbit IgG, goat IgG, streptavidin*			Dianova, Hamburg, Germany

[1] Matzku S, Wenzel A, Liu S, and Zöller M (1989). Antigenic differences between metastatic and nonmetastatic BSp73 rat tumor variants characterized by monoclonal antibodies. *Cancer Res* **49**, 1294–1299.

[2] Chang YW, Chen SC, Cheng EC, Ko YP, Lin YC, Kao YR, Tsay YG, Yang PC, Wu CW, and Roffler SR (2005). CD13 (aminopeptidase N) can associate with tumor-associated antigen L6 and enhance the motility of human lung cancer cells. *Int J Cancer* **116**, 243–252.

EAACC, European Association of Animal Cell Cultures (Porton Down, United Kingdom).

*Secondary antibodies and streptavidin were FITC, PE, biotin, or HRP labeled.

Table W2. List of Matrix Proteins.

Matrix Protein	Supplier	Concentration
Coll I	Sigma, Munich, Germany	10 μg/ml
Coll II	Sigma, Munich, Germany	10 μg/ml
Coll IV	Sigma, Munich, Germany	10 μg/ml
FN	Sigma, Munich, Germany	2 μg/ml
HA	Sigma, Munich, Germany	100 μg/ml
LN111	Sigma, Munich, Germany	1 μg/ml
LN332	804G [1] supernatant*	10 μg/ml
Vitronectin	Sigma, Munich, Germany	1 μg/ml
Matrigel	Becton Dickinson, Heidelberg, Germany	1:1 dilution

[1] Homma Y, Ozono S, Numata I, Seidenfeld J, and Oyasu R (1985). α-Difluoromethylornithine inhibits cell growth stimulated by a tumor-promoting rat urinary fraction. *Carcinogenesis* **6**, 159–161.

*804G cell culture supernatant was used as source of LN332. 804G cells were cultured (48 hours) in serum-free medium. Cleared supernatants (2 × 10 minutes, 500*g*; 1 × 20 minutes, 2000*g*; 1 × 30 minutes, 10,000*g*; 90 minutes, 100,000*g*) were centrifuged for vesicle depletion and concentrated. These serum-free, vesicle-depleted supernatants, highly enriched for LN332, are for brevity referred to as LN332.

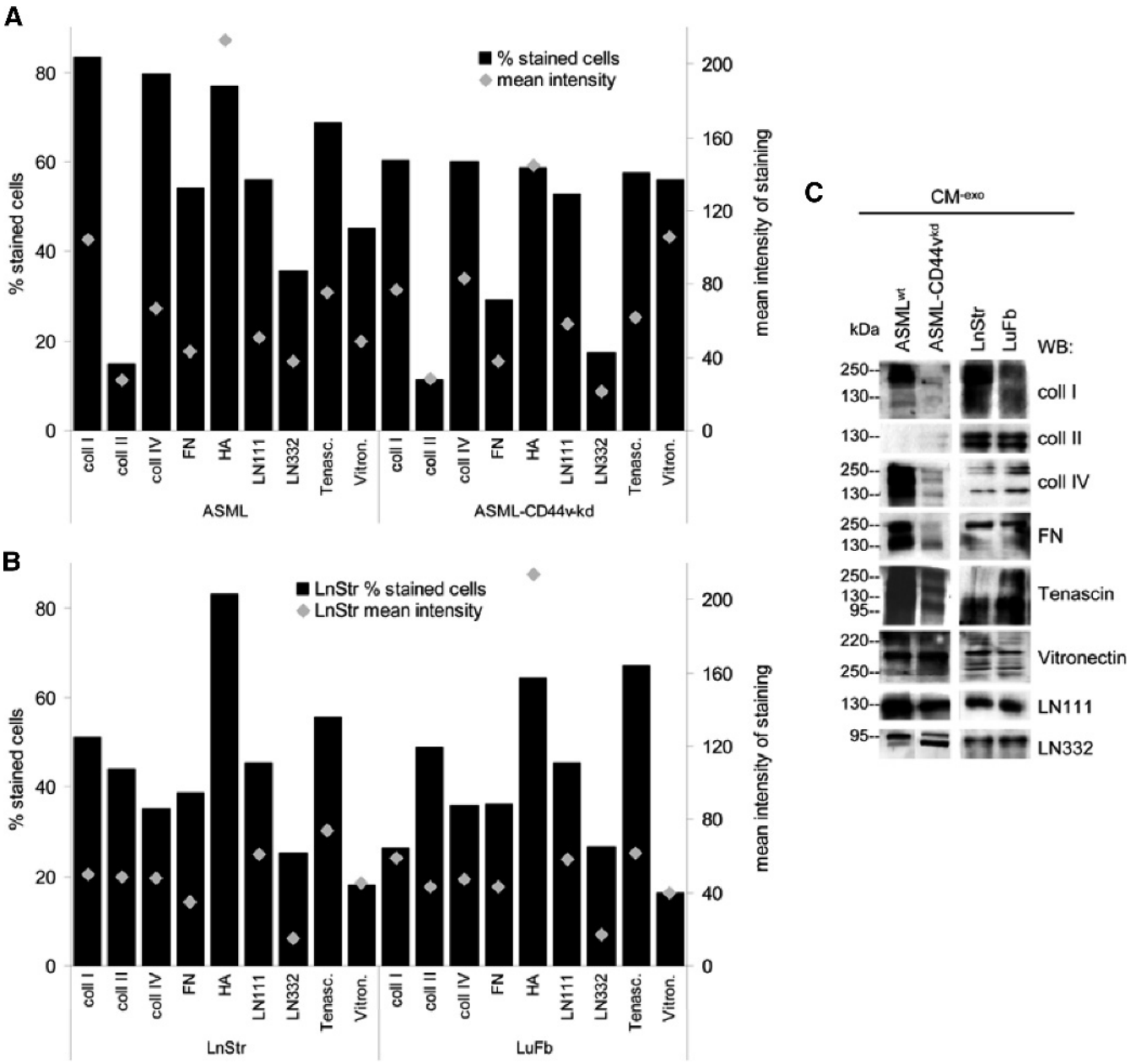

Figure W1. Recovery of matrix proteins in tumor and stroma cell CM. (A, B) ASML^{wt}, ASML-CD44v^{kd}, LnStr, and LuFb were stained with the indicated antibodies. The percent of stained cells and the intensity of staining were evaluated by flow cytometry. Mean values of triplicates are presented. (C) WB analysis of the indicated matrix proteins in CM^{-exo} of ASML^{wt}, ASML-CD44v^{kd}, LnStr, and LuFb.

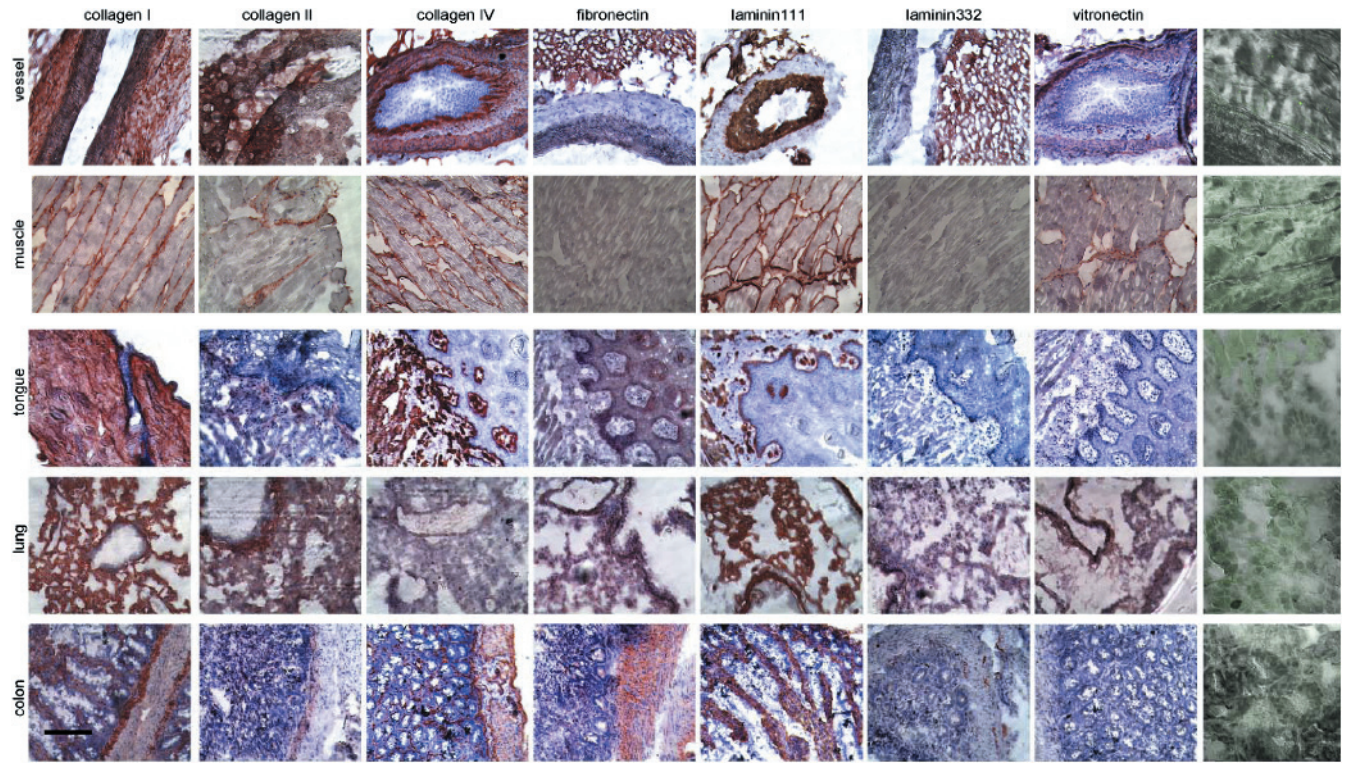

Figure W2. ECM proteins in different rat tissues: Rats received an i.v. injection of 200 μg of dye-labeled ASML^{wt} exosomes and were sacrificed after 48 hours (see Figure 1*E*). Sections of shock-frozen tissues were stained with the indicated antibodies and counterstained with H&E (scale bar, 100 μm). Recovery of dye-labeled exosomes is shown for comparison.

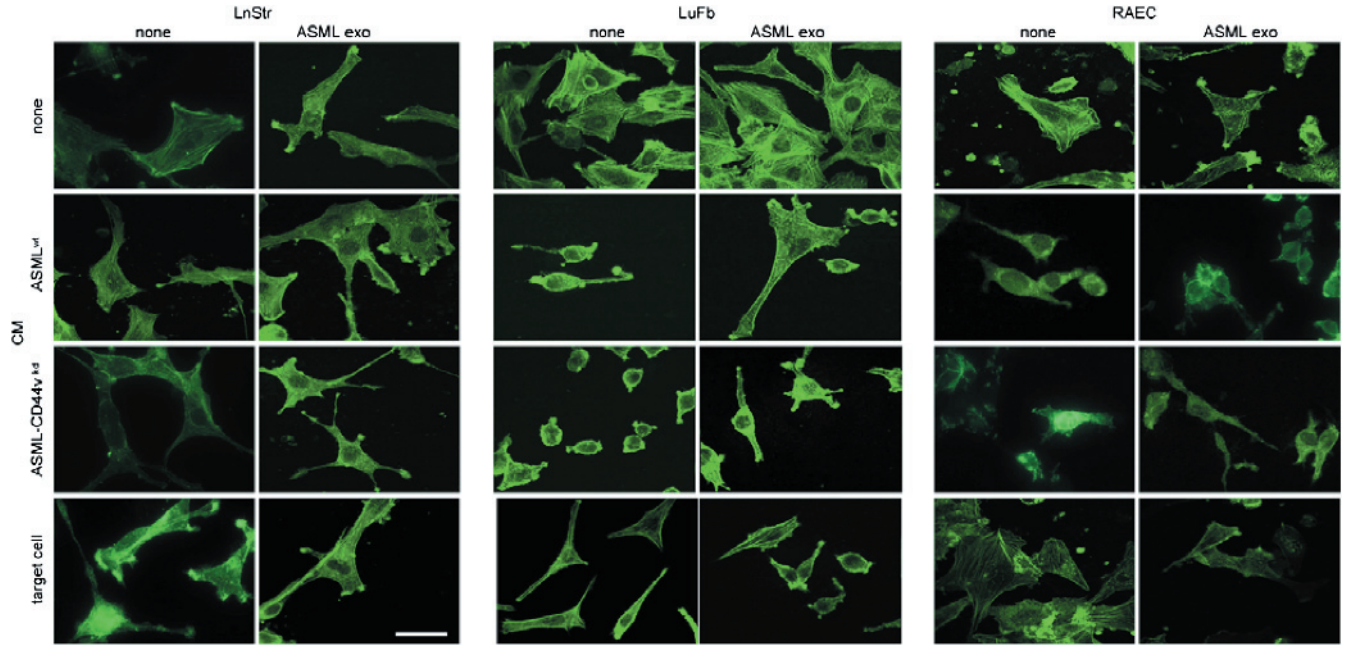

Figure W3. TEX-modulated CM and cell spreading: LnStr, LuFb, and RAEC were seeded on cover slides coated with BSA, ASML^{wt}, ASML-CD44v^{kd}, or target cell CM^{-exo}. Where indicated, the CM^{-exo} was pretreated with ASML^{wt} exosomes. Four hours after seeding, cells were stained with phalloidin-FITC. Staining was evaluated by confocal microscopy (scale bar, 10 μm). Representative examples are shown. ASML^{wt} and target cell CM promote cell spreading. ASML^{wt} exosome-treated CM supports the formation of focal adhesion clusters.

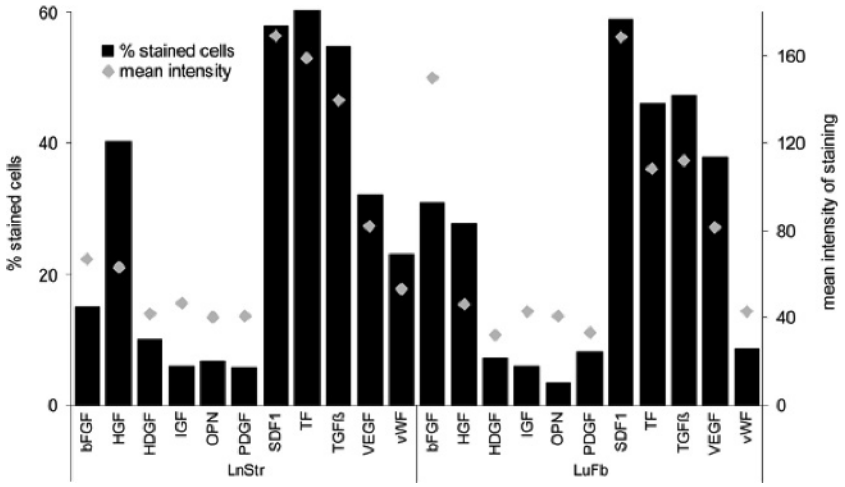

Figure W4. Cytokine and chemokine expression in stroma cells: Flow cytometry analysis of cytokine/chemokine expression in LnStr and LuFb cells. Mean values (three assays) of the percentage of stained cells and the mean intensity of staining are shown. LnStr and LuFb are rich in bFGF, HGF, SDF1, TF, and VEGF.